Applications of Mathematics

Olaf Klein

On forward and inverse uncertainty quantification for a model for a magneto mechanical device involving a hysteresis operator

Applications of Mathematics, Vol. 68 (2023), No. 6, 795–828

Persistent URL: http://dml.cz/dmlcz/151940

ON FORWARD AND INVERSE UNCERTAINTY QUANTIFICATION FOR A MODEL FOR A MAGNETO MECHANICAL DEVICE INVOLVING A HYSTERESIS OPERATOR

Olaf Klein, Berlin

Received March 31, 2023. Published online October 12, 2023.

Abstract. Modeling real world objects and processes one may have to deal with hysteresis effects but also with uncertainties. Following D. Davino, P. Krejčí, and C. Visone (2013), a model for a magnetostrictive material involving a generalized Prandtl-Ishlinskiĭ-operator is considered here.

Using results of measurements, some parameters in the model are determined and inverse Uncertainty Quantification (UQ) is used to determine random densities to describe the remaining parameters and their uncertainties. Afterwards, the results are used to perform forward UQ and to compare the generated outputs with measured data. This extends some of the results from O. Klein, D. Davino, and C. Visone (2020).

Keywords: hysteresis; uncertainty quantification (UQ); magnetostrictive material; Bayesian inverse problems (BIP)

MSC 2020: 47J40, 60H30

1. Uncertainty quantification and hysteresis: motivation and topics

1.1. Uncertainties in models with hysteresis operators. Considering magnetization, piezo-electric effects, elasto-plastic behavior, or magnetostrictive materials, one has to take into account hysteresis effects. Many models involve therefore *hysteresis operators* and are also subject to *uncertainties*:

- ▷ Parameters in the models are identified using results from *measurements*. Hence, they can be influenced by *measurement errors*.
- ▷ Parameters being identified for some *sample specimens* are also used for other specimens.

Open Access funding enabled and organized by Projekt DEAL.

DOI: 10.21136/AM.2023.0080-23

- ▷ Material/device may change after performing the measurements, for example, due to temperature changes or aging.
- ▷ Moreover, if one is performing several measurements, there can be conditions not considered in the model that change between the measurements, creating quite different measurement results that correspond to different parameter values in the used model.

The parameters in the hysteresis operators used to model hysteresis effects are therefore also subject to uncertainties. In the following, methods of *Uncertainty Quantification (UQ)* will be applied to describe/determine the uncertainties and to investigate their influence.

1.2. Uncertainty quantification. In view of e.g., [17], [18], the following interpretation of UQ is considered: Use of probability theory to deal with uncertainties, i.e., parameters with uncertain values are represented by random variables modeling the information/assumptions/beliefs on the values and the uncertainties of the parameter values. In the current paper, the following aspects of UQ will be discussed:

Forward UQ: Starting from representations of the uncertain parameter values by random variables, one considers the model output as random variable and computes properties like expected value, variation, probabilities for outputs entering some interval, credible intervals, and other *Quantities of Interest (QoI)*.

Inverse UQ: Using data and measurements to determine values and the uncertainty of the parameters, i.e., to determine a random variable taking into account the information provided by the data and the measurements, and use the random variable to represent the parameters afterwards.

Other subjects of/related to UQ, like *sensitivity analysis*, where one is investigating which input parameters have the largest effect (in terms of uncertainty) on the output quantity, will not be discussed here.

1.3. UQ for a model for magneto-mechanical components—topic of this paper. A model with a hysteresis operator is used to describe a magnetostrictive actuator. Using measurements for this actuator, parameters in the hysteresis operator and their uncertainty are identified by inverse UQ. Afterwards, forward UQ is performed. This work extends results from Section 5 in [7].

2. Hysteresis operators

2.1. Hysteresis operators—general definition. In this section, it is assumed that some $T > 0$ is given. Following [2], [10], [19], it is defined:

Definition 2.1. Let nonempty sets X, Y, and $\mathcal{H}\colon D(\mathcal{H}) \to \mathrm{Map}([0,T],Y)$ with $\emptyset \neq D(\mathcal{H}) \subseteq \mathrm{Map}([0,T],X)$ be given.

(a) $\mathcal{H}$ is a *hysteresis operator* $\Leftrightarrow$ $\mathcal{H}$ is rate-independent and causal.

(b) $\mathcal{H}$ is *rate-independent* $\Leftrightarrow$ for all $v \in D(\mathcal{H})$ for all $\alpha\colon [0,T] \to [0,T]$ being continuous and increasing (not necessary strictly increasing) with $\alpha(0) = 0$, $\alpha(T) = T$, and $v \circ \alpha \in D(\mathcal{H})$ it holds: $\mathcal{H}[v \circ \alpha] = \mathcal{H}[v] \circ \alpha$.

(c) $\mathcal{H}$ is *causal* $\Leftrightarrow$ for all $v_1, v_2 \in D(\mathcal{H})$ for all $t \in [0,T]$: If $v_1(\tau) = v_2(\tau)$ for all $\tau \in [0,t]$, then $\mathcal{H}[v_1](t) = \mathcal{H}[v_2](t)$.

2.2. The play-operator—definition and properties. The play-operator defined below is an important example of an hysteresis operator and is used to define further hysteresis operators.

Definition 2.2. Considering a *yield limit* $r \geqslant 0$ and an *initial state* $z \in \mathbb{R}$, the *play-operator* $\mathcal{P}_r[z,\cdot]$ maps $u \in C([0,T];\mathbb{R})$ being piecewise monotone to $\mathcal{P}_r[z,u] \in C([0,T];\mathbb{R})$ which is also piecewise monotone and it holds (see, e.g., [2], [9], [10], [19]) that

$$\mathcal{P}_r[z,u](0) = \max(u(0) - r, \min(u(0) + r, z)), \tag{2.1}$$

$$\mathcal{P}_r[z,u](t) = \begin{cases} \max(\mathcal{P}_r[z,u](t_*), u(t) - r) & \text{if } u \text{ is increasing on } [t_*,t], \\ \min(\mathcal{P}_r[z,u](t_*), u(t) + r) & \text{if } u \text{ is decreasing on } [t_*,t], \end{cases} \tag{2.2}$$

for all $t_*, t \in [0,T]$ with $t_* < t$ such that u *is monotone on* $[t_*,t]$.

As an example, the output of $\mathcal{P}_2[0,u]$ for an input function u is considered. The corresponding evolutions combined with plots for $u + 2$ and $u - 2$ are shown in Figure 1. Moreover, the corresponding input-output diagram, showing the evolution of $(u, \mathcal{P}_2[0,u])$, is presented in Figure 2.

Remark 2.3. Using e.g., [2], [9], [10], [19], one can show:

(a) It holds for all $r \geqslant 0$ and all $z \in \mathbb{R}$: the play-operator defined above can be continuously extended to the well known and well defined *play-operator* $\mathcal{P}_r[z,\cdot]$ from $\mathrm{C}([0,T];\mathbb{R})$ to $\mathrm{C}([0,T];\mathbb{R})$, being also a hysteresis operator.

(b) Let $\lambda_0\colon [0,\infty) \to \mathbb{R}$ being Lipschitz-continuous with Lipschitz constant 1 be given such that there exists some $R > 0$ with $\lambda_0(r) = 0$ for all $r \geqslant R$. Then

it holds for all $u \in \mathrm{C}([0,T];\mathbb{R})$ and all $t \in [0,T]$: the mapping $\mathcal{P}.[\lambda_0(\cdot),u](t)\colon [0,\infty) \to \mathbb{R}$ defined by $[0,\infty) \ni r \mapsto \mathcal{P}_r[\lambda_0(r),u](t)$ is continuous and there is some $R_{u,t} > 0$ such that $\mathcal{P}_r[\lambda_0(r),u](t) = 0$ for all $r > R_{u,t}$.

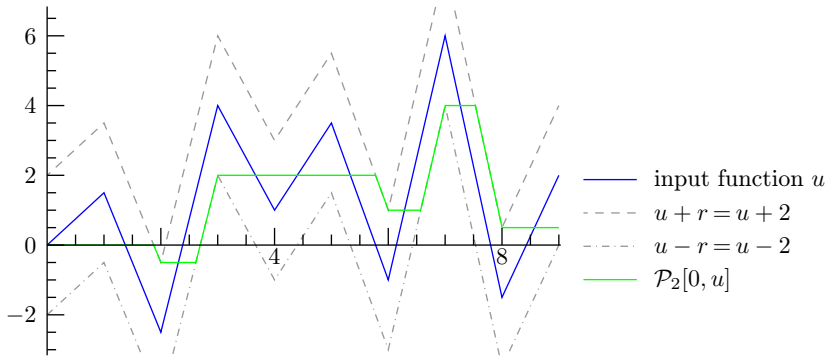

Figure 1. Evolution of the input $u(t)$, of $u(t) - 2$, of $u(t) + 2$, and of the output of the play-operator $\mathcal{P}_2[0,u](t)$.

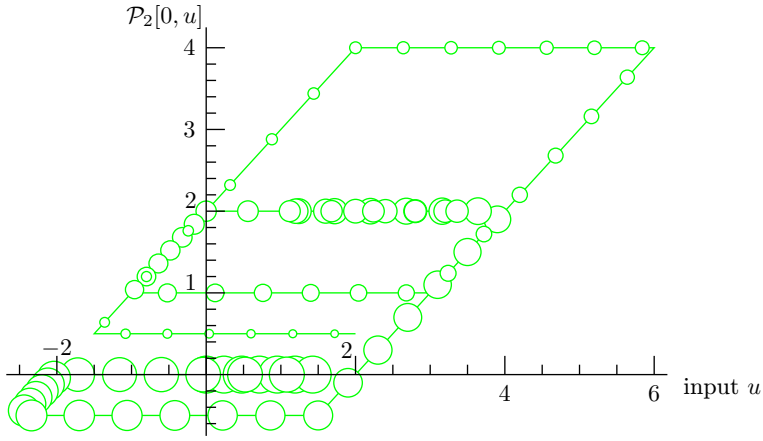

Figure 2. Input-output-diagram, derived using the data leading to Figure 1. Therein, the evolution of $(u(t), \mathcal{P}_2[0,u](t))$ is shown. The size of the circles is decreasing while t increases.

2.3. Prandtl-Ishlinskiĭ-operator. Following [2], [9], [10], [19], it is defined:

Definition 2.4. Let $\zeta \in L^1_{\mathrm{loc}}([0,\infty))$ be given.

(a) Let $\lambda_0\colon [0,\infty) \to \mathbb{R}$ being Lipschitz-continuous with Lipschitz constant 1 be given such that there exists some $R > 0$ with $\lambda_0(r) = 0$ for all $r \geqslant R$. Let $\mathcal{PI}_\zeta[\lambda_0,\cdot] : C([0,T];\mathbb{R}) \to C([0,T];\mathbb{R})$ be the *Prandtl-Ishlinskiĭ-operator for the weight function* ζ *and the initial state function* λ_0 defined by mapping $u \in$

$C([0,T];\mathbb{R})$ to the function $\mathcal{PI}_\zeta[\lambda_0,u]\in C([0,T];\mathbb{R})$ with

$$\mathcal{PI}_\zeta[\lambda_0,u](t)=\int_0^\infty \zeta(r)\mathcal{P}_r[\lambda_0(r),u](t)\,\mathrm{d}r \quad \forall\, t\in[0,T]. \tag{2.3}$$

(b) The *Prandtl-Ishlinskiĭ-operator* $\mathcal{PI}_\zeta[0,\cdot]$ *for the weight function* ζ *and the trivial initial state* is defined as the operator in a) with $\lambda_0\equiv 0$ on $[0,\infty)$.

(c) The *Prandtl-Ishlinskiĭ-operator* $\mathcal{PI}_\zeta[\cdot,\cdot]$ *for the weight function* ζ maps (λ_0,u) with λ_0 as in (a) and $u\in C([0,T];\mathbb{R})$ to $\mathcal{PI}_\zeta[\lambda_0,u]$ as in (a).

(d) The *initial loading curve* $\Psi_{\mathcal{PI},\zeta}(s)$ *for the Prandtl-Ishlinskiĭ-operator* $\mathcal{PI}_\zeta[\cdot,\cdot]$ is defined by requesting that for all $\beta\in\mathbb{R}$:

$$\Psi_{\mathcal{PI},\zeta}(\beta):=\mathcal{PI}_\zeta[0,u_\beta](T) \text{ with } u_\beta\in C([0,T];\mathbb{R}) \text{ defined by } u_\beta(t)=\beta\frac{t}{T} \quad \forall\, t\in[0,T]. \tag{2.4}$$

R e m a r k 2.5. Let $\zeta\in L^1_{\mathrm{loc}}([0,\infty))$ be given. For the initial loading curve $\Psi_{\mathcal{PI},\zeta}$ for the Prandtl-Ishlinskiĭ-operator $\mathcal{PI}_\zeta[\cdot,\cdot]$ it holds for all $s\in\mathbb{R}$ that

$$\begin{aligned}\Psi_{\mathcal{PI},\zeta}(s)&=\begin{cases}\displaystyle\int_0^s \zeta(r)(s-r)\,\mathrm{d}r & \text{if } s>0,\\ 0 & \text{if } s=0,\\ \displaystyle\int_0^{-s}\zeta(r)(s+r)\,\mathrm{d}r & \text{if } s<0,\end{cases}\\ &=-\Psi_{\mathcal{PI},\zeta}(-s).\end{aligned} \tag{2.5}$$

2.4. Identification of initial loading curve from measurements.

R e m a r k 2.6. Using [4], [11], [14], one can show: For $u\in C([0,T];\mathbb{R})$ and $0\leqslant t_a<t_b<t_c\leqslant T$ with u being monotone on $[t_a,t_b]$ and on $[t_b,t_c]$ and $u(t_a)=u(t_c)$ it holds that

$$\forall\, t\in[t_b,t_c]\colon\ \Psi_{\mathcal{PI},\zeta}\Big(\frac{u(t)-u(t_b)}{2}\Big)=\frac{1}{2}(\mathcal{PI}_\zeta[\lambda_0,u](t)-\mathcal{PI}_\zeta[\lambda_0,u](t_b)). \tag{2.6}$$

R e m a r k 2.7. If one is considering a process mapping time-dependent input functions to a measurable time-dependent output quantity Q, then one may like to model this by applying a Prandtl-Ishlinskiĭ-operator. To identify a corresponding weight function, one can use a function u with a cycle as in Remark 2.6 as an input to this process and determine given/measured values for u and Q at times $s_0<s_1<\ldots<s_K$ with $t_b=s_0$ and $s_K=t_c$. Hence, one gets $0=v_0<v_1<\ldots<v_K$ and $\psi_0,\psi_1,\ldots,\psi_K\in\mathbb{R}$ defined by

$$v_i:=\Big|\frac{u(s_i)-u(s_0)}{2}\Big|,\quad \psi_i:=\frac{1}{2}\begin{cases}Q(s_i)-Q(s_0) & \text{if } u(s_K)\geqslant u(s_0),\\ Q(s_0)-Q(s_i) & \text{if } u(s_K)\leqslant u(s_0).\end{cases} \tag{2.7}$$

By recalling (2.6), it can be deduced that one is looking for a weight function ζ with

$$\Psi_{\mathcal{PI},\zeta}(v_i) \approx \psi_i \quad \forall\, i \in \{0,\dots,K\}. \tag{2.8}$$

Since the definition yields that $v_0 = 0$ and $\psi_0 = 0$, it is deduced from (2.5) that the equation in (2.8) is satisfied for $k = 0$ for all admissible weight functions ζ such that for determining ζ one can ignore $k = 0$ in (2.8).

R e m a r k 2.8. Starting from data as in Remark 2.7 one can derive an approximation for an initial loading curve on $[0, v_K]$ by considering a function Ψ that is linear on $[v_0, v_1]$, $[v_1, v_2], \dots, [v_{K-1}, v_K]$ and satisfies $\Psi(v_k) = \psi_k$ for all $k \in \{0,\dots,K\}$.

R e m a r k 2.9. The considerations in Remark 2.7 can be extended to the following situation: one is considering a function $u \in C([0,T];\mathbb{R})$ and $t_b, t_c \in [0,T]$ with $t_b < t_c$ such that u is monotone on $[t_b, t_c]$ and one is able to show somehow that the equation in (2.6) is at least approximately valid for all $t \in [t_b, t_c]$.

3. Uncertainties in a model for magneto-mechanical components

3.1. General considerations. In [3], Section 5, a model for magneto-mechanical devices has been derived. Therein, a *generalized Prandtl-Ishlinskiĭ-operator*, see also [8], [20],

$$\mathcal{G}_{c_1,c_2,c_3}[\lambda_0, H](t) := \mathcal{PI}_{\zeta_{c_1,c_2}}[\lambda_0, \tanh(c_3 H)](t) \tag{3.1}$$

with $\zeta_{c_1,c_2}(r) := c_1 \mathrm{e}^{-r/c_2}$ for all $r \geqslant 0$, parameters $c_1, c_2, c_3 > 0$ and $\lambda_0 \colon [0,\infty) \to \mathbb{R}$ satisfying the conditions discussed above, is considered. In [3], it is shown that this operator provides an approximation for the *magnetization* of Galfenol for an applied magnetic field H; with c_3 depending on the applied stress.

In the following, it will be assumed that the applied magnetic field H is proportional to the applied current I such that one can consider $\mathcal{G}_{c_1,c_2,c_3}[\lambda_0, I]$ (with an appropriate updated value for c_3) instead of $\mathcal{G}_{c_1,c_2,c_3}[\lambda_0, H]$.

The initial loading curve $\Psi_{\mathcal{PI},\zeta_{c_1,c_2}}$ for $\mathcal{PI}_{\zeta_{c_1,c_2}}$ satisfies

$$\Psi_{c_1,c_2}(s) := \Psi_{\mathcal{PI},\zeta_{c_1,c_2}}(s) = s c_1 c_2 + c_1 c_2^2 (\mathrm{e}^{-s/c_2} - 1) \quad \forall\, s \geqslant 0. \tag{3.2}$$

In [1], a magnetostrictive Terfenol-actuator is investigated and the hysteresis between the current generating the magnetic field and the resulting displacement is considered. In this paper, data creating a *First-Order-Reversal-Curves* (FORC)—diagram quite similar to the one in Figure 3 were used to determine the parameter field/values in a Preisach-operator and a generalized Prandtl-Ishlinskiĭ-operator.

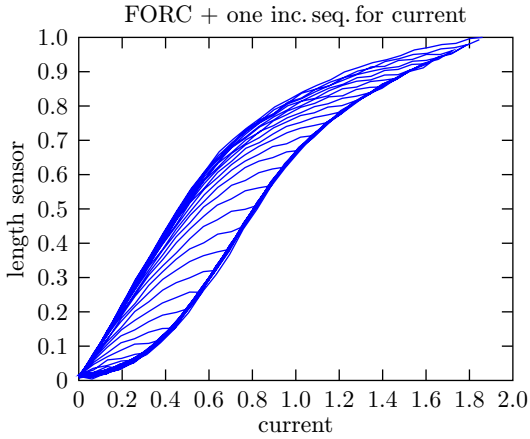

Figure 3. A FORC-diagram for a magnetostrictive Terfenol-actuator similar to the one considered in [1], and one additional curve derived for increasing current.

3.2. Considerations and results in [7], Section 5. The data used to prepare the FORC-diagram in Figure 3 and one additional data set with increasing current measured directly afterward are shown in Figure 4. In [7], Section 5, these data have been used to identify parameter values $c_1, c_2, c_3 > 0$ such that the generalized Prandtl-Ishlinskiĭ-operator $\mathcal{G}_{c_1,c_2,c_3}[\lambda_0, I](t)$ creates approximations for these data. The resulting value for $c_3 = c_{\tanh} = 0.682138$ will be used in the following. Moreover, the uncertainties for c_1 and c_2 were also investigated.

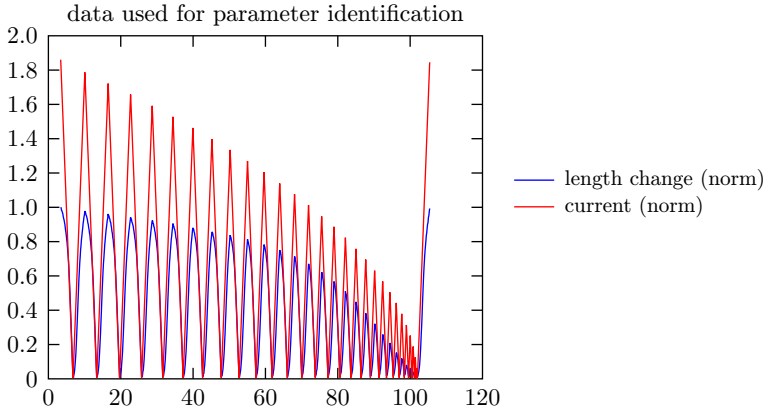

Figure 4. Measured data used to generate the FORC-diagram in Figure 3, and one additional data set with increasing current measured directly afterwards.

In the following, let $t_0, t_1, \ldots, t_{58}$ denote the times of local extrema for the current I. The symbol L will be the relative length change determined from measurements of a corresponding sensor. Thanks to the measurements, there are values for I

and L at times $s_{0,j}, s_{1,j}, \dots s_{K_j^*,j} \in [t_{j-1}, t_j]$ with $t_{j-1} = s_{0,j} < s_{1,j} < \dots < s_{K_j^*,j} = t_j$ for all $j \in \{1, \dots, 58\}$ and

$$K_1^* = 29, \quad K_2^* = K_3^* = 28, \quad K_4^* = K_5^* = 27, \dots, K_{54}^* = K_{55}^* = 2, \\ K_{56} = 1, \quad K_{57} = 2, \quad K_{58} = 29. \tag{3.3}$$

In the following, results from a reformulation of Section 2 will be used. In this reformulation every "$[0, T]$" is replaced with "$[t_0, t_{58}]$", "$\alpha(0) = 0$" and "$\alpha(T) = T$" in Definition 2.1 (b) are replaced with "$\alpha(t_0) = t_0$" and "$\alpha(t_{58}) = t_{58}$", respectively, "$[0, t]$" in Definition 2.1 (c) is replaced with "$[t_0, t]$", "0" in (2.1) is replaced with "t_0", and "$0 \leqslant t_a < t_b < t_c \leqslant T$" in Remark 2.6 is replaced with "$t_0 \leqslant t_a < t_b < t_c \leqslant t_{58}$".

Considering any $j \in \{2, \dots, 57\}$ and investigating the evolution of $u := \tanh(c_3 I)$ on $[t_{j-2}, t_{j-1}]$ and on $[t_{j-1}, t_j]$, it follows that one is dealing with the situation discussed in Remark 2.6 with $t_{j-2} =: t_a$, $t_{j-1} =: t_b$ and $t_j =: t_c$.

For any $i \in \{1, \dots, 28\}$, it holds that u is increasing on $[t_{2i-1}, t_{2i}] = [s_{0,2i}, s_{K_i,2i}]$ with $K_i := K_{2i}^*$. Hence, by following Remark 2.7, one can compute $v_{0,i}, \dots, v_{K_i,i}$ and $\psi_{0,i}, \dots, \psi_{K_i,i}$ defined by

$$\begin{aligned} v_{k,i} &:= \frac{1}{2} |\tanh(c_3 I(s_{k,2i})) - \tanh(c_3 I(s_{0,2i}))| \\ &= \frac{1}{2} (\tanh(c_3 I(s_{k,2i})) - \tanh(c_3 I(s_{0,2i}))), \\ \psi_{k,i} &:= \frac{1}{2} (L(s_{k,2i}) - L(s_{0,2i})), \end{aligned} \tag{3.4}$$

for $k = 0, \dots, K_i$. Now, in view of (2.6) and (2.8), one would like to find density ζ_i for the Prandtl-Ishlinskiĭ-operator such that

$$\Psi_{\mathcal{PI},\zeta_i}(v_{k,i}) \approx \psi_{k,i} \quad \forall\, k \in \{0, \dots, K_i\}. \tag{3.5}$$

Moreover, one can either combine the return point memory property of the Prandtl-Ishlinskiĭ operator with its continuity or investigate the graphs $[0, \infty) \ni r \mapsto \mathcal{P}_r[\lambda_0(r), u](t)$ and compute the resulting integrals to show for $t_b := t_{57}$ and $t_c := t_{58}$ that one is in a situation as in Remark 2.9. Hence, equations (3.4) and (3.5) can also be derived for $i = 29$ with $K_{29} := K_{2\cdot 29}^* = K_{58}^*$.

For any $i \in \{31, \dots, 58\}$, it holds that u is decreasing on $[t_{2(i-30)}, t_{2(i-30)+1}] = [s_{0,2(i-30)+1}, s_{K_i,2(i-30)+1}]$ with $K_i := K_{2(i-30)+1}^*$ and that one is in the situation discussed in Remark 2.6. Hence, by following this remark, one can compute

$v_{0,i}, \dots, v_{K_i,i}$ and $\psi_{0,i}, \dots, \psi_{K_i,i}$ by

$$
\begin{aligned}
v_{k,i} &:= \frac{1}{2}|\tanh(c_3 I(s_{k,2(i-30)+1})) - \tanh(c_3 I(s_{0,2(i-30)+1}))| \\
&= \frac{1}{2}(\tanh(c_3 I(s_{0,2(i-30)+1})) - \tanh(c_3 I(s_{k,2(i-30)+1}))), \\
\psi_{k,i} &:= \frac{1}{2}(L(s_{0,2(i-30)+1}) - L(s_{k,2(i-30)+1})),
\end{aligned} \tag{3.6}
$$

for $k = 0, \dots, K_i$. Now, again in view of (2.6) and (2.8), one would like to find density ζ_i for the Prandtl-Ishlinskiĭ-operator such that $\Psi_{\mathcal{PI},\zeta_i}(v_{k,i}) \approx \psi_{k,i}$ for all $k \in \{0, \dots, K_i\}$.

Moreover, since the experiment is supposed to generate measurements allowing to generate a FORC-diagram, it can be assumed that the preparation phase of the measurement has been done in such a way that (2.6) is valid with $t_b := t_0 = t_{2(30-30)}$ and $t_c := t_1 = t_{2(30-30)+1}$, such that the above considerations can also be performed for $i = 30$.

Combining the above considerations, it holds for any $j \in \{1, \dots, 58\}$ that K_j, $v_{0,j}, \dots, v_{K_j,j}$, and $\psi_{0,j}, \dots, \psi_{K_j,j}$ have been determined such that one would like to find density ζ_j for the Prandtl-Ishlinskiĭ-operator satisfying

$$
\Psi_{\mathcal{PI},\zeta_j}(v_{k,j}) \approx \psi_{k,j} \quad \forall\, k \in \{0, \dots, K_j\}. \tag{3.7}
$$

Following Remark 2.8, an approximation for an initial loading curve can also be derived from this data set. In Figure 5, these approximations are shown.

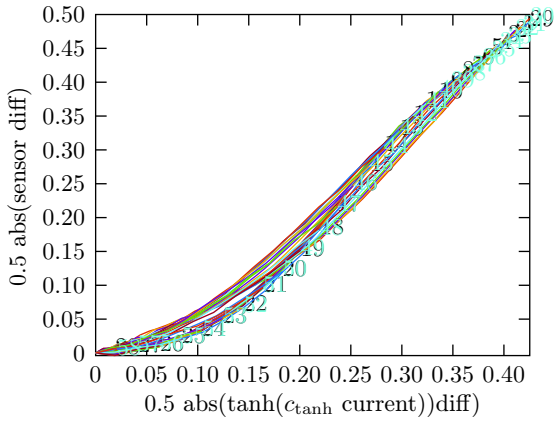

Figure 5. For every $i \in \{1, 2, \dots, 58\}$ the approximation of an initial loading curve generated from points $(v_{0,i}, \psi_{0,i}), (v_{1,i}, \psi_{1,i}), \dots, (v_{K_i,i}, \psi_{K_i,i})$ following Remark 2.8 is shown.

As pointed out before (2.8), for determining ζ_j one can ignore $k = 0$ in the above equation. If one is only interested in dealing with densities as in Section 3.1, one has $\zeta_j = \zeta_{c_{1,j},c_{2,j}}$ with appropriate values $c_{1,j}, c_{2,j} \in (0, \infty)$ so that it holds, thanks to (3.2),

$$\Psi_{c_{1,j},c_{2,j}}(v_{k,j}) \approx \psi_{k,j} \quad \forall\, k \in \{1, \dots, K_j\}. \tag{3.8}$$

R e m a r k 3.1. In [7], Section 5, appropriate pairs

$$(c_{1,KDV,1}, c_{2,KDV,1}), (c_{1,KDV,2}, c_{2,KDV,2}), \dots, (c_{1,KDV,58}, c_{2,KDV,58})$$

were computed such that (3.8) is satisfied for $c_{1,j} = c_{1,KDV,j}$ and $c_{2,j} = c_{2,KDV,j}$ for all $j \in \{1, \dots, 58\}$. Afterwards, a simple inverse UQ calculation was performed: for a subset

$$((c_{1,KDV,i}, c_{2,KDV,i}))_{i=30}^{55}$$

of nice parameter pairs the discrete mean and the standard deviation were calculated. Afterwards, c_1 and c_2 were represented by independent random variables with the corresponding normal distributions truncated to $[0.0000001, \infty)$ and some forward UQ computations were performed.

Performing a further simple inverse UQ by also computing the discrete mean and the discrete standard deviation using all pairs $((c_{1,KDV,i}, c_{2,KDV,i}))_{i=1}^{58}$, it turned out that the discrete mean for c_2 was 4.71742 and the discrete standard deviation for c_2 was 7.94603, so that using a truncated normally distributed distribution does not seem to be an appropriate description for c_2. Moreover, it turned out that the values in $((c_{1,KDV,i}, c_{2,KDV,i}))_{i=1}^{58}$ show a significant correlation and considering their distribution (see [7], Figure 14), it became obvious that these pairs do not represent samples of two independent truncated normally distributed random variables.

Also, the values in the subset $((c_{1,KDV,i}, c_{2,KDV,i}))_{i=30}^{55}$ of nice parameter pairs show a significant correlation and investigating the distribution of these pairs, see [7], Figure 15, it became obvious that these pairs also do not represent samples of two independent truncated normally distributed random variables.

Because of these observations, it was tried in [7], Section 5 to find a random variable on $(0, \infty)^2$ such that the above pairs could be typical samples for this random variable, by applying a formulation of Bayes' Theorem as in [6], Theorem 3.1, see also Section 3.4.

3.3. Likelihood and Bayes' Theorem. The following definition of the likelihood (compare, e.g., [17], [16], [6]) is quite often applied in situations with V_q being equal to the value of a model evaluated at q with additional noise that is normally distributed with mean 0.

Definition 3.2. Let $m, n \in \mathbb{N}$ be given. Let $Q \subset \mathbb{R}^m$ be a set of parameter values. Assume that for every $q \in Q$ a continuous $\mathbb{R}^n$-valued random variable V_q with probability density $\varrho(\cdot; q)$ on $\mathbb{R}^n$ is given. For all $q \in Q$ and all $v \in \mathbb{R}^n$ it holds that the *likelihood* $L(q \mid v)$ is defined by

$$L(q \mid v) := \varrho(v; q) = \varrho(V_q = v; q). \tag{3.9}$$

The *likelihood function* $L(\cdot \mid v)$ for v is mapping $q \in Q$ to $L(q \mid v)$.

This combination of assumptions is used in the following:

Assumption 3.3. Assume that one is in the situation of Definition 3.2 and that integrals on Q are well defined. Assume that a known probability density π_0 on Q, denoted as *prior density*, is given. Assume that some $v_{\text{obs}} \in \bigcup_{q \in Q} V_q$ is given such that $\int_Q L(q' \mid v_{\text{obs}}) \pi_0(q') \, \mathrm{d}q' > 0$.

Having a close look at the proof of [6], Theorem 3.1, one realizes that the first equation on page 51 only holds if therein the density of the to be identified random variable representing the parameters is replaced by the prior density. Adapting now the corresponding formulation of *Bayes' Theorem of Inverse Problems* such that the proof is valid, one ends up with the following theorem allowing to compute the solution of the corresponding *Bayesian Inverse Problems* (BIP) with (3.10). Similar formulations can also be found e.g., in [17], Result 8.1 or [12], Section 2.1.2.

Theorem 3.4. *Assume that Assumption* 3.3 *is satisfied and that a random variable X_0 with values in Q is given such that π_0 is its probability density, that v_{obs} can be considered as a sample of V_{X_0} and that there exists a joint probability density for X_0 and V_{X_0}. A Baysian's belief π_{new} combining the information in X_0 and in the observed datum v_{obs} is the posterior probability density $\pi_{\text{new}}(\cdot \mid V_{X_0} = v_{\text{obs}})$ of X_0, given the data v_{obs}, and it holds that*

$$\pi_{\text{new}}(q \mid V_{X_0} = v_{\text{obs}}) = \frac{L(q \mid v_{\text{obs}}) \pi_0(q)}{\int_Q L(q' \mid v_{\text{obs}}) \pi_0(q') \, \mathrm{d}q'} \quad \forall \, q \in X_0. \tag{3.10}$$

In [18], Section 6.22, the formulation of Bayes' Theorem of Inverse Problems is adjusted to the situation that Q is a subset of a general separable Banach space and V_q is of the form described before Definition 3.2.

As one can see, the derived density does not depend on X_0, so that the following theorem is proved.

Theorem 3.5. *Assume that Assumption* 3.3 *is satisfied and that a random variable X_0 with values in Q exits such that the assumptions in Theorem* 3.4 *are satisfied.*

A Baysian's belief combining the information in π_0 and in the observed datum v_{obs} by using Bayes' Theorem of Inverse Problems is the posterior probability density for the prior density π_0, given the data v_{obs} which is defined as the posterior probability density $\pi_{\text{new}}(\cdot \mid V_{X_0} = v_{\text{obs}})$ of X_0, given the data v_{obs} as in Theorem 3.4.

R e m a r k 3.6. Assume that Assumption 3.3 is satisfied and that one tries to identify a fixed, true, and unknown value $q_{\text{true}} \in Q$. Assume that the informations/beliefs on the value of q_{true} in advance of an observation are summarized by the *prior* probability density π_0 on Q. Assume that v_{obs} is a sample of $V_{q_{\text{true}}}$ that has been observed. A Baysian's belief combining the information in π_0 and in the observed datum v_{obs} by using Bayes' Theorem of Inverse Problems as in Theorem 3.5 is the *posterior probability density for the prior density π_0, given the data v_{obs}*. This density is defined following Theorem 3.5 if it holds that there exists a random variable X_0 with values in Q such that the assumptions in Theorem 3.4 are satisfied. (This implies that one needs to request that v_{obs} is also a sample of V_{X_0}.)

R e m a r k 3.7. For the "identification of a true value" formulation of Bayes' Theorem as in Remark 3.6 one can subsequently apply the theorem for different observations, using the last computed posterior density as new prior density. In this situation one can show some kind of convergence of the computed densities to the true value with the Bernstein-von Mises Theorem (see, e.g., [18], Theorem 6.17). Hence, this yields that in most situations the posterior density computed by Bayes' Theorem provides better approximation to the true value than the prior density.

R e m a r k 3.8. In some references, e.g., [6], Theorem 3.1, a more general situation than in Remark 3.6 seems to be considered. Therein, the authors claim to deal with the situation that there is a *fixed, true random variable* U_{true} with values in Q, such that the observations are samples of $V_{U_{\text{true}}}$. If one has a *prior* probability density π_0 on Q representing the information on/beliefs about U_{true} in advance of the observation(s), it is pointed out that for any observed datum v_{obs} of this kind one can use Bayes' Theorem of Inverse Problems as in Theorem 3.5 to get the posterior probability density for the prior density π_0, given the data v_{obs}.

Warning: The posterior density one gets in this situation is the *same* as the posterior density one would get if considering Bayes' Theorem for the identification of a true value as in Remark 3.6. There are some situations, in which the computed posterior density can be a better approximation for U_{true} than the prior density, but contrary to the expectation, this does *not* hold typically. Instead, one can easily produce situations with a given and known U_{true} such that the posterior density is the *less accurate* approximation of U_{true} especially if V_q is of the form described before Definition 3.2.

3.4. Adapting the identification problem to Bayes' Theorem. Adapting the situation considered in Section 3.2 to the framework of Bayes' Theorem, it is assumed that there exist independent random variables $\Gamma_{1,1},\dots,\Gamma_{K_1,1},\Gamma_{1,2},\dots,\Gamma_{K_2,2},\dots,\Gamma_{1,L},\dots,\Gamma_{K_L,L}$ and samples $\gamma_{k,l}$ of $\Gamma_{k,l}$ such that (3.8) can be rewritten as

$$\Psi_{\mathcal{PI},c_{1,l},c_{2,l}}(v_{k,l})+\gamma_{k,l}=\psi_{k,l}\quad \forall\, k\in\{1,\dots,K_l\},\ l\in\{1,\dots,L\}. \tag{3.11}$$

In [7] it is assumed that $\Gamma_{2,1},\dots,\Gamma_{K_1,1},\Gamma_{2,2},\dots,\Gamma_{K_2,2},\dots,\Gamma_{2,L},\dots,\Gamma_{K_L,L}$ have the distribution $N(0,\sigma^2)$ and that $\Gamma_{1,1},\Gamma_{1,2},\dots,\Gamma_{1,L}$ have the distribution $\mathcal{N}(0,(2\sigma)^2)$ for a given σ.

In view of the formulation of Bayes' Theorem as in [6], Theorem 3.1, see also Remark 3.8, it was believed that appropriate application of Bayes' Theorem should allow the determination of a posterior density such that $((c_{1,KDV,i},c_{2,KDV,i}))_{i=1}^{58}$ as in Remark 3.1 could be considered as typical samples for a random variable with this density. An idea to achieve this aim was to subsequently apply Bayes' theorem to (3.11) for the different values of $l\in\{1,2,\dots,58\}$, using the last computed posterior density as new prior density in each step.

But an inspection of this procedure yielded that the resulting final posterior density can also be derived by applying Bayes' Theorem just with the likelihood being the product of all involved likelihoods, leading to a density for (c_1,c_2).

Considering the likelihoods for $\sigma=0.01$ and $\sigma=0.02$, shown in [7], Figures 16, and 17, one observes that these functions are very small except for a quite small region, but the values for $((c_{1,KDV,i},c_{2,KDV,i}))_{i=1}^{58}$ are distributed over a much larger region, see [7], Figure 14. The pairs in the considered subset $((c_{1,KDV,i},c_{2,KDV,i}))_{i=30}^{55}$ of nice parameter pairs are also distributed over a much larger region, see [7], Figure 15.

Hence, with a normal choice for the prior density considered during the application of Bayes' Theorem it will also hold that the posterior density is concentrated in a small region and a random variable with this density will not produce one of these sets of parameter values as typical samples.

In view of these results, further investigation of the application of Bayes' Theorem was performed. It turned out that the posterior density computed by using this product of likelihoods is just the density that one would get for $c_{1,\mathrm{all}},c_{2,\mathrm{all}}\in(0,\infty)$ such that (3.11) holds with $c_{1,l}$ replaced by $c_{1,\mathrm{all}}$ and $c_{2,l}$ replaced by $c_{2,\mathrm{all}}$ for all $l\in\{1,\dots,58\}$, see also the Warning in Remark 3.8.

4. Inverse and forward UQ computations performed after completing [7]

4.1. Reformulation of problems to be considered for Bayes' Theorem, use of UQLab. In the following, Bayes' Theorem will be applied for appropriate parts of the BIP considered before and afterwards a convex combination of the resulting posterior densities will be determined.

To be able to deal with the posterior density and integrals involving this density, this density will be represented by samples resulting from dealing with BIPs using Markov-Chain-Monte-Carlo (MCMC)-computations. This has been done by applying *UQLab*, the *"The Framework for Uncertainty Quantification"*, see [13], [21] and `https://www.uqlab.com/`.

For subsets $\mathfrak{L}$ of $\{1,2,\dots,L\}=\{1,2,\dots,58\}$, it will be assumed that for all $l\in\mathfrak{L}$ it holds that the corresponding equations in (3.11) are evaluated with $c_{1,l}$ replaced by $c_{1,\mathfrak{L}}$ and $c_{2,l}$ replaced by $c_{2,\mathfrak{L}}$. Hence, it can be deduced that

$$\Psi_{\mathcal{PI},c_{1,\mathfrak{L}},c_{2,\mathfrak{L}}}(v_{k,l})+\gamma_{k,l}=\psi_{k,l}\quad\forall\, k\in\{1,\dots,K_l\},\ l\in\mathfrak{L}. \tag{4.1}$$

Moreover, it will be assumed that the independent random variables $\Gamma_{k,l}$ have the distribution $\mathcal{N}(0,\sigma^2_{\mathfrak{L}})$ for all $k\in\{1,\dots,K_l\}$ and for all $l\in\mathfrak{L}$ with some appropriate $\sigma_{\mathfrak{L}}>0$ that must be identified.

Hence, it follows that $(\psi_{k,l})_{k=1,\dots,K_l,l\in\mathfrak{L}}$ can be considered as sample of

$$(\Psi_{\mathcal{PI},c_{1,\mathfrak{L}},c2,\mathfrak{L}}(v_{k,l})+\Gamma_{k,l})_{k=1,\dots,K_l,\,l\in\mathfrak{L}}.$$

Therefore, similarly to [21], (1.17), it holds for the likelihood that

$$\begin{aligned}L_{\mathfrak{L}}((c_{1,\mathfrak{L}},c_{2,\mathfrak{L}},\sigma^2_{\mathfrak{L}})\mid(\psi_{k,l})_{k=1,\dots,K_l,\,l\in\mathfrak{L}})\\ =\prod_{l\in\mathfrak{L}}\prod_{k=1}^{K_l}\frac{1}{\sqrt{2\pi\sigma^2_{\mathfrak{L}}}}\exp\Big(\frac{-1}{2\sigma^2_{\mathfrak{L}}}(\psi_{k,l}-\Psi_{\mathcal{PI},c_{1,\mathfrak{L}},c_{2,\mathfrak{L}}}(v_{k,l}))^2\Big).\end{aligned} \tag{4.2}$$

4.2. Approximation of length change and shift value. If one plans to use the results of inverse UQ to perform forward UQ and to reconstruct the measured length change, it is important to take into account the following considerations:

If one is considering a triple c_1,c_2,c_3 and would like to construct an approximation of the measured length change, it holds:

Variant 1: One could try to identify the initial internal state λ_0 describing the internal state of the specimen before the measurement started that corresponds to the 0-length change situation such that $\mathcal{G}_{c_1,c_2,c_3}[\lambda_0,I]$ with a shift should reproduce the measurements.

Variant 2: One could take advantage of the fact that in the situation considered in the measurements (also after the identification period is finished) it holds that there is a constant difference between $\mathcal{G}_{c_1,c_2,c_3}[\lambda_0, I]$ and $\mathcal{G}_{c_1,c_2,c_3}[0, I]$, with $\mathcal{G}_{c_1,c_2,c_3}[0, I]$ denoting the generalized Prandtl-Ishlinskiĭ-operator involving the Prandtl-Ishlinskiĭ-operator with a trivial initial state as in Definition 2.4 (b). Then, one just needs to determine a shift-value such that $\mathcal{G}_{c_1,c_2,c_3}[0, I] + \text{shift}$ is an approximation for the measured length change.

In the following, Variant 2 will be used and the value for shift will be determined by computing the output of the generalized Prandtl-Ishlinskiĭ-operator with a trivial initial state at a time t being a minimum, i.e., $t \in \{t_1, t_3, \dots, t_{57}\}$, and comparing the result with the measured length change $L(t)$ at this time.

R e m a r k 4.1. If one is investigating the properties of the play-operator with a trivial initial state with the modification that t_0 is the start of the considered time interval, see the discussions of the reformulation of Section 2 in Section 3.2, it holds that

$$\mathcal{G}_{c_1,c_2,c_3}[0, I](t_0) = \mathcal{PI}_{\zeta_{c_1,c_2}}[0, \tanh(c_3 I)](t_0) = \Psi_{c_1,c_2}(\tanh(c_3 I(t_0))). \tag{4.3}$$

Moreover, following the discussion for the derivation of (3.7) for $i = 30$, it can be deduced that (2.6) is valid with $t_b = t_0$, $t = t_1$, and $u = \tanh(c_3 I)$. Using also (2.5) and simplifying the notations by using that the value of c_3 is fixed, it follows that

$$\mathcal{G}_{c_1,c_2,c_3}[0, I](t_1) = g_{c_1,c_2}(t_1) \tag{4.4}$$

with

(4.5)
$$\begin{aligned} g_{c_1,c_2}(t) := {} & \Psi_{c_1,c_2}(\tanh(c_3 I(t_0))) \\ & + 2\Psi_{\mathcal{PI},c_{1,\mathfrak{L}},c_{2,\mathfrak{L}}}\Big(\frac{1}{2}(\tanh(c_3 I(t)) - \tanh(c_3 I(t_0)))\Big) \quad \forall\, t \in [t_0, t_{58}]. \end{aligned}$$

Taking advantage of the return-point memory of the generalized Prandtl-Ishlinskiĭ-operator and ignoring that there may be some differences, since the values of the minima have some small variations, it follows that

$$\mathcal{G}_{c_1,c_2,c_3}[0, I](t_i) \approx g_{c_1,c_2}(t_i) \quad \forall\, i \in \{1, 3, 5, \dots, 57\}. \tag{4.6}$$

Now, considering the situation as in Section 4.1 for a subset $\mathfrak{L}$ of $\{1, \dots, L\}$, one equation or several equations involving $\text{shift}_{\mathfrak{L}}$ and one or several measurements of length changes needs/need to be formulated.

When doing forward UQ by considering samples representing the unknown parameters one also needs to somehow determine samples for $\text{shift}_{\mathfrak{L}}$.

Variant 1: If only one equation involving $\mathrm{shift}_{\mathfrak{L}}$ is formulated, the following simple approach was used in previous computations: In the first step, one can perform inverse UQ using the likelihood formulated in Section 4.1 to generate a set of sample triples $((c_{1,\mathfrak{L},n}, c_{2,\mathfrak{L},n}, \sigma^2_{\mathfrak{L},n}))_{n=1}^N$ representing the joint posterior density for $c_{1,\mathfrak{L}}$, $c_{2,\mathfrak{L}}$, and $\sigma^2_{\mathfrak{L}}$. In the second step, one computes for each pair $(c_{1,\mathfrak{L},n}, c_{2,\mathfrak{L},n})$ the corresponding sample value $\mathrm{shift}_{\mathfrak{L},n}$ by inverting the equation discussed above. Afterwards, one could consider the quadruple of samples $((c_{1,\mathfrak{L},n}, c_{2,\mathfrak{L},n}, \mathrm{shift}_{\mathfrak{L},n}, \sigma^2_{\mathfrak{L},n}))_{n=1}^N$ as samples of some joint density representing $c_{1,\mathfrak{L}}$, $c_{2,\mathfrak{L}}$, $\mathrm{shift}_{\mathfrak{L}}$, and $\sigma^2_{\mathfrak{L}}$.

Variant 2: The more complicated approach is to perform the inverse UQ already with $\mathrm{shift}_{\mathfrak{L}}$ as a component and to use also the equation(s) for the shift value in the formulation of the BIP. In the following, results for these kind of computations are presented.

To derive a BIP combining (4.1) with an equation for $\mathrm{shift}_{\mathfrak{L}}$, one needs to formulate one equation or several equations for this quantity such that the error can be estimated. Moreover, to implement this within the framework of UQLab, one needs to formulate equations such that the error should be a sample of a random variable having the distribution $\mathcal{N}(0, \sigma^2_{\mathfrak{L}})$.

To prepare this, one will consider the times for minima belonging to the data sets used to create $((v_{k,l}, \psi_{k,l}))_{k=1,\dots,K_l,\, l\in\mathfrak{L}}$. Hence,

$$\mathfrak{L}^* := \{2i \mid i \in \mathfrak{L},\ i \leqslant 29\} \cup \{2(i-30)+1 \mid i \in \mathfrak{L},\ i \geqslant 30\} \tag{4.7}$$

is considered. Now, it is assumed that

$$\eta^*_{k,j,\mathfrak{L}} := \mathcal{G}_{c_1,c_2,c_3}[0,I](s_{k,j}) + \mathrm{shift}_{\mathfrak{L}} - L(s_{k,j}) \tag{4.8}$$

for $k \in \{0,\dots,K^*_j\}$ and for $j \in \mathfrak{L}^*$ are samples for independent random variables all having the distribution $\mathcal{N}(0, \sigma^2_{\mathfrak{L},*})$ for some appropriate $\sigma_{\mathfrak{L},*} > 0$. (Here, it is ignored that in view of (4.9) and other already requested independencies one may not be able to satisfy all the requested independencies.) Considering any $l \in \mathfrak{L}$ with $l < 29$ and any $k \in \{1,\dots,K_l\}$ and recalling (4.1), (3.4), and (2.6) allows to deduce that

(4.9)

$$\begin{aligned}
\gamma_{k,l} &= \frac{1}{2}(L(s_{k,2l}) - L(s_{0,2l})) - \Psi_{\mathcal{PI},c_{1,\mathfrak{L}},c_{2,\mathfrak{L}}}\Big(\frac{1}{2}(\tanh(c_3 I(s_{k,2l})) - \tanh(c_3 I(s_{0,2l})))\Big) \\
&= \frac{1}{2}(L(s_{k,2l}) - \mathcal{G}_{c_{1,\mathfrak{L}},c_{2,\mathfrak{L}},c_3}[0,I](s_{k,2l}) - \mathrm{shift}_{\mathfrak{L}}) \\
&\quad - \frac{1}{2}(L(s_{0,2l}) - \mathcal{G}_{c_{1,\mathfrak{L}},c_{2,\mathfrak{L}},c_3}[0,I](s_{0,2l}) - \mathrm{shift}_{\mathfrak{L}}) \\
&= -\frac{1}{2}\eta^*_{k,2l,\mathfrak{L}} + \frac{1}{2}\eta^*_{0,2l,\mathfrak{L}}.
\end{aligned}$$

Using further argumentation similar to the one that was used to derive equations (3.4) and (3.5) also for $i = 29$, it can be shown that (4.9) is also valid for $l = 29$.

Recalling the assumption for $\eta^*_{i,2l,\mathfrak{L}}$ and Lemma 6.1, see Appendix, yields that the difference on the right-hand side of (4.9) is a sample of a random variable with distribution $N\big(0, \big(\frac{1}{\sqrt{2}}\sigma_{\mathfrak{L},*}\big)^2\big)$, and that this therefore also holds for $\gamma_{k,l}$.

Considering any $l \in \mathfrak{L}$ with $l > 29$ and any $k \in \{1, \dots, K_l\}$ and recalling (4.1), (3.6), and (2.6) allows to deduce with a similar computation that $\gamma_{k,l} = -\frac{1}{2}\eta^*_{0,2(l-30)+1,\mathfrak{L}} + \frac{1}{2}\eta^*_{k,2(l-30)+1,\mathfrak{L}}$. Recalling the assumption for $\eta^*_{i,2(l-30)+1,\mathfrak{L}}$ and Lemma 6.1, one deduces that this is a sample of a random variable with distribution $N\big(0, \big(\frac{1}{\sqrt{2}}\sigma_{\mathfrak{L},*}\big)^2\big)$.

Since it holds for all $l \in \mathfrak{L}$ and all $k \in \{1, \dots, K_l\}$ that $\gamma_{k,l}$ is by assumption a sample of a random variable with distribution $N(0, \sigma^2_{\mathfrak{L}})$, but also a sample of a random variable with distribution $N\big(0, \big(\frac{1}{\sqrt{2}}\sigma_{\mathfrak{L},*}\big)^2\big)$, it follows that

$$\frac{1}{\sqrt{2}}\sigma_{\mathfrak{L},*} = \sigma_{\mathfrak{L}}. \tag{4.10}$$

4.3. Bayesian Inverse Problem for data sets with increasing current. Considering the approximation for initial loading curves generated by following Remark 2.8 for the data sets with increasing current, as shown in Figure 6, one observes that they all seem to approximate the same function on different intervals.

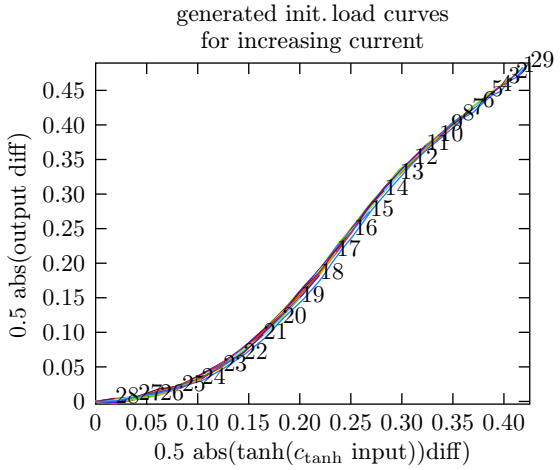

Figure 6. For the data sets involving increasing current, i.e., for every $i \in \{1, 2, \dots, 29\}$, the approximation of an initial loading curve generated from the points $(v_{0,i}, \psi_{0,i})$, $(v_{1,i}, \psi_{1,i}), \dots, (v_{K_i,i}, \psi_{K_i,i})$ following Remark 2.8 is shown.

To get samples representing the approximation of this function, a BIP for all data sets with increasing current is considered, i.e., one deals with $\mathfrak{L} = \{1, \dots, 29\}$. Using (4.7), it follows that $\mathfrak{L}^* = \{2, 4, \dots, 58\}$.

Equation for shift: In a situation without any noise or any model errors, one could compute the average over all values for $\mathcal{G}_{c_1,c_2,c_3}[0,I]$ evaluated in the 29 minima of the current at $t_1, t_3, \ldots, t_{57}$ and afterwards add $\text{shift}_{\{1,\ldots,29\}}$ to this average. The result should be equal to the average over all values for L evaluated in the 29 minima of the current.

In a situation with noise, one needs to consider the difference between these expressions and one has to check if it can be considered as a sample of a random variable. Denoting the difference by $\delta_{\{1,\ldots,29\}}$, it follows that

$$\begin{aligned}\delta_{\{1,\ldots,29\}} &= \frac{1}{29}\sum_{i=1}^{29}\mathcal{G}_{c_1,c_2,c_3}[0,I](t_{2i-1}) + \text{shift}_{\{1,\ldots,29\}} - \frac{1}{29}\sum_{i=1}^{29}L(t_{2i-1}) \\ &= \frac{1}{29}\sum_{i=1}^{29}(\mathcal{G}_{c_1,c_2,c_3}[0,I](s_{0,2i}) + \text{shift}_{\{1,\ldots,29\}} - L(s_{0,2i})) = \sum_{i=1}^{29}\frac{1}{29}\eta^*_{0,2i,\{1,2,\ldots,29\}}.\end{aligned}$$

Recalling Lemma 6.1, the assumption on $\eta^*_{0,2i,\{1,2,\ldots,29\}}$, and (4.10), it is shown that the sum on the right-hand side is a sample for a random variable with distribution $\mathcal{N}\Big(0, \sum_{i=1}^{29}(\frac{1}{29})^2\sigma^2_{\{1,2,\ldots,29\},*}\Big) = \mathcal{N}\big(0, \frac{1}{29}\sigma^2_{\{1,2,\ldots,29\},*}\big) = \mathcal{N}\big(0, \frac{2}{29}\sigma^2_{\{1,2,\ldots,29\}}\big)$. In view of Lemma 6.1, it can be deduced that $\sqrt{\frac{29}{2}}\delta_{\{1,\ldots,29\}}$ would be a sample of a random variable with distribution $\mathcal{N}\big(0,\sigma^2_{\{1,2,\ldots,29\}}\big)$. Hence, using also (4.6), it follows that $\sqrt{\frac{29}{2}}\frac{1}{29}\sum_{i=1}^{29}L(t_{2i-1})$ is a sample of a random variable with distribution $\mathcal{N}\Big(\sqrt{\frac{29}{2}}\Big(\frac{1}{29}\Big(\sum_{i=1}^{29}g_{c_1,c_2}(t_{2i-1})\Big) + \text{shift}_{\{1,\ldots,29\}}\Big), \sigma^2_{\{1,2,\ldots,29\}}\Big)$.

Attaching this random variable to $(\Psi_{\mathcal{PI},c_1,\mathfrak{L},c_2,\mathfrak{L}}(v_{k,l}) + \Gamma_{k,l})_{k=1,\ldots,K_l,\,l=1,\ldots,29}$, ignoring in the following computations that the involved random variables are not independent, and considering (4.2) with $\mathfrak{L} = \{1,2,\ldots,29\}$, it follows for the resulting likelihood that

(4.11)

$$\begin{aligned}&L^{\text{full}}_{\{1,2,\ldots,29\}}((c_{1,\{1,2,\ldots,29\}}, c_{2,\{1,2,\ldots,29\}}, \text{shift}_{\{1,2,\ldots,29\}}, \sigma^2_{\{1,2,\ldots,29\}}) \mid \\ &\qquad ((\psi_{k,l})_{k=1,\ldots,K_l,\,l=1,\ldots,29}, \Upsilon)) \\ &\quad = L_{\{1,2,\ldots,29\}}((c_{1,\{1,2,\ldots,29\}}, c_{2,\{1,2,\ldots,29\}}, \sigma^2_{\{1,2,\ldots,29\}}) \mid (\psi_{k,l})_{k=1,\ldots,K_l,\,l=1,2,\ldots,29}) \\ &\qquad \times L^*_{\{1,2,\ldots,29\}}((c_{1,\{1,2,\ldots,29\}}, c_{2,\{1,2,\ldots,29\}}, \text{shift}_{\{1,2,\ldots,29\}}, \sigma^2_{\{1,2,\ldots,29\}}) \mid \Upsilon),\end{aligned}$$

where

$$\Upsilon = \sqrt{\frac{29}{2}}\frac{1}{29}\sum_{i=1}^{29}L(t_{2i-1})$$

and

$$
\begin{aligned}
(4.12)\qquad & L^*_{\{1,2,\dots,29\}}((c_{1,\{1,2,\dots,29\}}, c_{2,\{1,2,\dots,29\}}, \mathrm{shift}_{\{1,2,\dots,29\}}, \sigma^2_{\{1,2,\dots,29\}}) \mid \Upsilon) \\
&\quad = \frac{1}{\sqrt{2\pi\sigma^2_{\{1,2,\dots,29\}}}} \exp\Bigg(\frac{-1}{4 \cdot 29\sigma^2_{\{1,2,\dots,29\}}} \Bigg(\sum_{i=1}^{29} L(t_{2i-1}) \\
&\qquad - \sum_{i=1}^{29} g_{c_{1,\{1,2,\dots,29\}}, c_{2,\{1,2,\dots,29\}}}(t_{2i-1}) - 29\,\mathrm{shift}_{\{1,2,\dots,29\}} \Bigg)^2 \Bigg).
\end{aligned}
$$

Now, the product of appropriate uniform probability densities for $c_{1,\{1,2,\dots,29\}}$, $c_{2,\{1,2,\dots,29\}}$, $\mathrm{shift}_{\{1,2,\dots,29\}}$, and $\sigma^2_{\{1,2,\dots,29\}}$ is used as prior density. Ignoring that the prior density should not involve any information derived by using the observations to be considered in Bayes' Theorem, the data pairs $((c_{1,KDV,i}, c_{2,KDV,k}))_{i=1}^{58}$ and the subset $((c_{1,KDV,i}, c_{2,KDV,k}))_{i=30}^{55}$ of nice data pairs computed in [7], Section 5 by using this observation, see Remark 3.1, have been used to define the prior density. Moreover, the results of other inverse UQ computations for the considered observation have also been used.

(1) The interval $[0, 100]$ used for $c_{1,\{1,2,\dots,29\}}$ is chosen so that all values $(c_{1,KDV,i})_{i=30}^{55}$ and almost all values $(c_{1,KDV,i})_{i=31}^{58}$ are within this interval.

(2) The interval $[0.00001, 4]$ used for $c_{2,\{1,2,\dots,29\}}$ satisfies that most of the values $(c_{2,KDV,i})_{i=30}^{55}$ and many of the values for $(c_{2,KDV,i})_{i=1}^{58}$ are within this interval. The used upper bound 4 for $c_{2,\{1,2,\dots,29\}}$ was derived by some heuristic considerations to ensure that there is still some reasonable dependence of $L_{\{1,2,\dots,29\}}((c_1, c_2, \sigma^2) \mid (\psi_{k,l})_{k=1,2,\dots,K_l, l=1,2,\dots,29})$ on c_2 on the complete interval.

(3) Using data pairs for (c_1, c_2) derived by performing inverse UQ without the shift, and computing the shift by inverting the considered equation, many samples for shift had been computed. The interval $[-3, 3]$ contains almost all of them.

(4) In view of other results for dealing with the considered problem, using the interval $[0, 10^{-3}]$ to define the prior density for $\sigma^2_{\{1,2,\dots,29\}}$ seemed reasonable.

Following Remark 3.6, one is interested in the posterior density according to Bayes' Theorem of Inverse Problems as in Theorem 3.5.

To approximate the resulting posterior density a set of samples is computed by using the *affine invariant ensemble algorithm*, see [21], Section 1.3.4, a special Markov-Chain-Monte-Carlo scheme, implemented in UQLab. An ensemble of 200 chains, denoted as *walkers*, was considered, and 6000 iteration steps were performed. Afterwards, some walkers with improper evolutions were removed and the initial 90 % of the iterations steps in the remaining walkers were also removed. Hence, one got samples $((c_{1,\{1,2,\dots,29\},n}, c_{2,\{1,2,\dots,29\},n}, \mathrm{shift}_{\{1,2,\dots,29\},n}, \sigma^2_{\{1,2,\dots,29\},n}))_{n=1}^{115800}$.

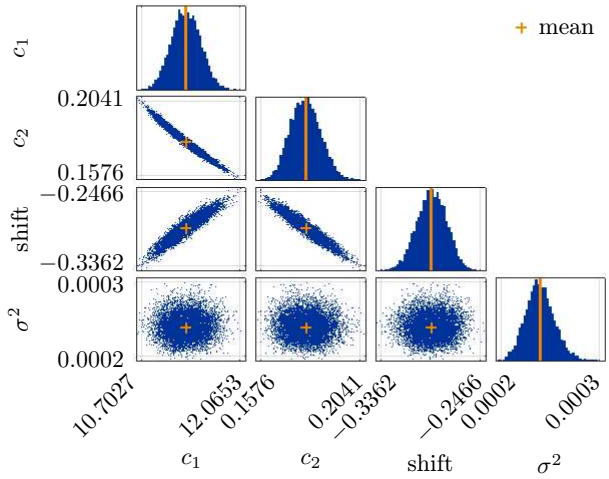

Figure 7. Scatter plot showing the samples $(c_{1,\{1,2,\ldots,29\},n}, c_{2,\{1,2,\ldots,29\},n}, \text{shift}_{\{1,2,\ldots,29\},n}, \sigma^2_{\{1,2,\ldots,29\},n})$ representing the posterior density following from dealing with all data sets for increasing current.

These samples, i.e., a sufficient number of samples randomly selected from these samples, are presented in the scatter plot in Figure 7.

4.4. Result of forward UQ for data sets with increasing current. As pointed out in [21], the *posterior predictive density* can be computed by "averaging" the model output with additional noise over the posterior distribution. Thanks to (3.3) and Gauss summation, it follows that this is a density with $\sum_{l=1}^{29} K_l + 1 = \sum_{l=1}^{29} K^*_{2l} + 1 = \sum_{l=1}^{29} l + 1 = \frac{29*30}{2} + 1 = 436$ components.

Following [21], Section 1.2.6, one can generate samples for the posterior predictive density: Starting with a sample $(c_{1,\{1,2,\ldots,29\},n}, c_{2,\{1,2,\ldots,29\},n}, \text{shift}_{\{1,2,\ldots,29\},n}, \sigma^2_{\{1,2,\ldots,29\},n})$ reflecting the posterior density, one gets a sample $\xi_n \in \mathbb{R}^{436}$ reflecting the posterior predictive density by the following computation.

▷ Considering an index $k^* \in \{1, \ldots, 435\}$, one defines

$$l := \min\left\{ l^* \in \{1, \ldots, 29\} \,\middle|\, \sum_{i=1}^{l^*} K_i \geqslant k^* \right\}$$

and afterwards one defines $k = k^*$ if $l = 1$, and $k = k^* - \sum_{i=1}^{l-1} K_i$ otherwise. Now, $\xi_n(k^*)$ will be the sum of $\Psi_{c_{1,\{1,\ldots,29\},n}, c_{2,\{1,\ldots,29\},n}}(v_{k,l})$ and a sample of a random variable with distribution $\mathcal{N}(0, \sigma^2_{\{1,\ldots,29\},n})$.

▷ Moreover, $\xi_n(436)$ will be the sum of

$$\sqrt{\frac{29}{2}}\left(\frac{1}{29}\left(\sum_{i=1}^{29} g_{c_{1,\{1,\ldots,29\},n},c_{2,\{2,\ldots,29\},n}}(t_{2i-1})\right) + \text{shift}_{\{1,\ldots,29\}}\right)$$

and a sample of a random variable with distribution $\mathcal{N}\big(0, \sigma^2_{\{1,\ldots,29\},n}\big)$.

The considered data vector is

$$(\psi_{1,1}, \ldots, \psi_{K_1,1}, \psi_{1,2}, \ldots, \psi_{K_2,2}, \ldots, \psi_{1,29}, \ldots, \psi_{K_{29},29}, \Upsilon).$$

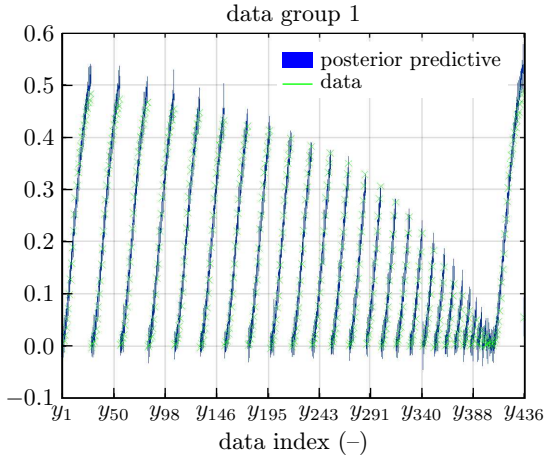

Figure 8. Violin-plots of samples reflecting the posterior predictive density, derived by using some of the samples shown in Figure 7 and marks for data points.

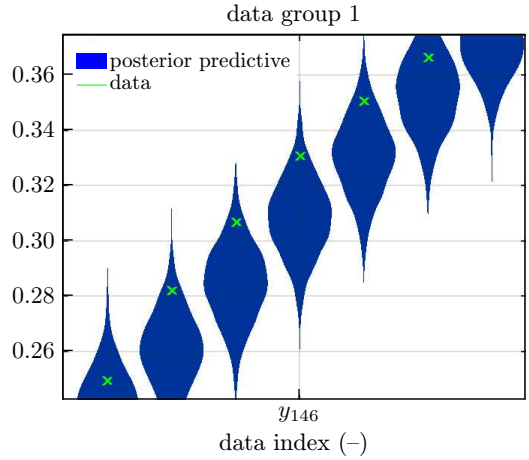

Figure 9. Blow-up of a part of Figure 8.

To plot the posterior predictive density, one is randomly choosing 1000 samples $(\xi_{n_i})_{i=1}^{1000}$, and is showing a violin-plot for $(\xi_{n_i}(k))_{i=1}^{1000}$ for each $k \in \{1, \ldots, 436\}$, see [15], Section uq_violinplot. In the plot, marks for the value of the components of the data vector are also shown. In Figure 8 this is shown for all 436 components, in the blow-up in Figure 9 one can see the result for the components $143, \ldots, 149$.

4.5. Bayesian Inverse Problems for data sets with decreasing current. Considering the approximation for initial loading curves generated for data sets with decreasing current, it can be observed that the curves look different, see Figure 10.

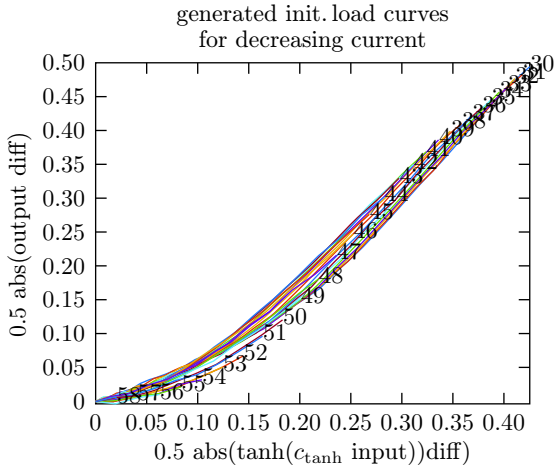

Figure 10. For the data sets involving decreasing current, i.e., for every $i \in \{30, 31, \ldots, 58\}$ the approximation of an initial loading curve generated from the points $(v_{0,i}, \psi_{0,i}), (v_{1,i}, \psi_{1,i}), \ldots, (v_{K_i,i}, \psi_{K_i,i})$ following Remark 2.8 is shown.

To get samples representing the approximation of these different functions, 29 Bayesian Inverse Problems are considered, one per each data set with decreasing current.

Let any $i \in \{30, \ldots, 58\}$ be given. Considering now $\mathfrak{L} = \{i\}$, it follows from (4.7) that $\mathfrak{L}^* = \{2(i-30)+1\}$.

Equation for $\text{shift}_{\{i\}}$: The data set $((v_{k,i}, \psi_{k,i}))_{k=1}^{K}$ is derived from information on the current and the length change on the interval $[t_{2(i-30)}, t_{2(i-30)+1}]$. Since the current is decreasing on this interval, it is minimal at the end $t_{2(i-30)+1} = s_{K_i,2(i-30)+1}$ of the interval.

Since $\eta^*_{K_i,2(i-30)+1,\{i\}}$ is a sample of a random variable having the distribution $\mathcal{N}(0, \sigma^2_{\{i\},*})$, it follows by recalling Lemma 6.1 and (4.10) that $\frac{1}{\sqrt{2}}\eta^*_{K_i,2(i-30)+1,\{i\}}$ is a sample of a random variable having the distribution $\mathcal{N}(0, \sigma^2_{\{i\}})$. Considering (4.8) for $k = K_i = K^*_{2(i-30)+1}$ and (4.6), it can be deduced that $\frac{1}{\sqrt{2}}L(t_{2(i-30)+1})$ is a sample

of a random variable with distribution $\mathcal{N}\big(\frac{1}{\sqrt{2}}(g_{c_{1,\{i\}},c_{2,\{i\}}}(t_{2(i-30)+1})+\mathrm{shift}_{\{i\}}),\sigma^2_{\{i\}}\big)$. Attaching this random variable to $(\Psi_{\mathcal{PI},c_{1,\{i\}},c_{2,\{i\}}{}_2}(v_{k,i})+\Gamma_{k,i})_{k=1}^{K_i}$, ignoring in the following computations that the involved random variables are not independent, and considering (4.2) with $\mathfrak{L}=\{i\}$, one gets for the resulting likelihood

$$
\begin{aligned}
(4.13)\quad & L^{\mathrm{full}}_{\{i\}}\Big((c_{1,\{i\}},c_{2,\{i\}},\mathrm{shift}_{\{i\}},\sigma^2_{\{i\}})\,\Big|\,\Big((\psi_{k,i})_{k=1}^{K_i},\frac{1}{\sqrt{2}}L(t_{2(i-30)+1})\Big)\Big)\\
&\qquad = L_{\{i\}}((c_{1,\{i\}},c_{2,\{i\}},\sigma^2_{\{i\}})\mid(\psi_{k,i})_{k=1}^{K_i})\\
&\qquad\quad \times L^*_{\{i\}}\Big((c_{1,\{i\}},c_{2,\{i\}},\mathrm{shift}_{\{i\}},\sigma^2_{\{i\}})\,\Big|\,\frac{1}{\sqrt{2}}L(t_{2(i-30)+1})\Big)
\end{aligned}
$$

with

(4.14)

$$
\begin{aligned}
&L^*_{\{i\}}\Big((c_{1,\{i\}},c_{2,\{i\}},\mathrm{shift}_{\{i\}},\sigma^2_{\{i\}})\,\Big|\,\frac{1}{\sqrt{2}}L(t_{2(i-30)+1})\Big)\\
&\quad=\frac{1}{\sqrt{2\pi\sigma^2_{\{i\}}}}\exp\Big(\frac{-1}{4\sigma^2_{\{i\}}}(L(t_{2(i-30)+1})-g_{c_{1,\{i\}},c_{2,\{i\}}}(t_{2(i-30)+1})-\mathrm{shift}_{\{i\}})^2\Big).
\end{aligned}
$$

As in Section 4.3, the product of appropriate uniform probability densities for $c_{1,\{i\}}$, $c_{2,\{i\}}$, $\mathrm{shift}_{\{i\}}$, and $\sigma^2_{\{i\}}$ is used as prior density. Moreover, similarly to Section 4.3, the interval $[0,100]$ is used for $c_{1,\{i\}}$, the interval $[-3,3]$ is used for $\mathrm{shift}_{\{i\}}$, and the interval $[0,10^{-3}]$ is used for $\sigma^2_{\{i\}}$.

The interval $[0.00001,c_{2,\mathrm{up},\{i\}}]$ is used for $c_{2,\{i\}}$ with an upper bound $c_{2,\mathrm{up},\{i\}}$ derived by some heuristic considerations to ensure that there is still a reasonable dependence of $L_{\{i\}}((c_1,c_2,\sigma^2)\mid(\psi_{k,l})_{k=1}^{K_i})$ on c_2 on the complete interval. It holds that $c_{2,\mathrm{up},\{30\}}=4$, $c_{2,\mathrm{up},\{40\}}=3.29284$, $c_{2,\mathrm{up},\{50\}}=1.76305$, $c_{2,\mathrm{up},\{58\}}=0.200779$.

As in Section 4.3, following Remark 3.6, one is interested in the posterior density according to Bayes' Theorem of Inverse Problems as in Theorem 3.5. Again, the affine invariant ensemble algorithm implemented in UQLab is applied.

In the first series of computations it turned out that for some values of i there are problems with the convergence of the algorithm; it seemed that the scheme was not able to find the region wherein the corresponding likelihood is not very small, since this region is much smaller than the overall considered domain.

Hence, to support the algorithm somehow, it was decided that the starting values for the walkers should no longer be determined using samples of the random variable having the prior density and is therefore uniform on $[0,100]\times[0.00001,c_{2,\mathrm{up},\{i\}}]\times[-3,3]\times[0,10^{-3}]$.

Instead, these initial values for the walkers were defined as the values of the walkers at the end of computations for an appropriate BIP performed as preparation. In this BIP it is requested that (4.1) is valid for $\mathfrak{L}=\{30,\dots,58\}$. Moreover, it is requested

in this BIP that the result of an incorrect derivation of the equation for shift in Section 4.3 applies, wherein it is assumed incorrectly that $\delta_{\{1,\dots,29\}}$ is a sample for a random variable with distribution $\mathcal{N}\big(0, \sigma^2_{\{1,2,\dots,29\},*}\big)$. The resulting modification of the likelihood in (4.12) multiplied by $\prod_{l=30}^{58} L_{\{l\}}\big(\big(c_{1,\{30,\dots,58\}}, c_{2,\{30,\dots,58\}}, \sigma^2_{\{30,\dots,58\}}\big) \mid (\psi_{k,l})_{k=1}^{K_l}\big)$ results in the likelihood considered for dealing with this intermediate BIP. This BIP is considered with the prior density as for $i = 1$, being the same as the one considered in Section 4.3. This intermediate BIP is solved by applying the affine invariant ensemble algorithm with 200 walkers and 6000 iteration steps.

After removing 5 walkers with improper evolutions, the final values of the remaining 195 walkers were stored. These values were afterwards used as starting values for the 195 walkers used when the algorithm was applied to deal with the BIP derived above for $\mathfrak{L} = \{i\}$.

4.6. Results of inverse and of forward UQ for the first data set for decreasing current. Results of inverse UQ for the first data set with decreasing current, i.e., the data set No. 30, are samples $(c_{1,\{30\},n}, c_{2,\{30\},n}, \text{shift}_{\{30\},n}, \sigma^2_{\{30\},n})$ as shown in Figure 11.

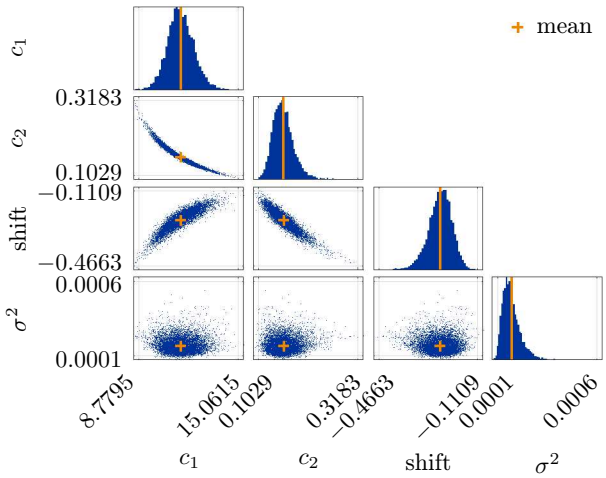

Figure 11. Resulting scatter plot of parameter samples $(c_{1,\{30\},n}, c_{2,\{30\},n}, \text{shift}_{\{30\},n}, \sigma^2_{\{30\},n})$ for the first data set with decreasing current, i.e., the data set No. 30.

Similarly to Section 4.4, samples for the posterior predictive density can be generated: Dealing with the first data set with decreasing current, i.e., with data set No. 30, it holds that the posterior predictive density has $K_{30} + 1 = 29 + 1 = 30$ components.

Starting from a sample $(c_{1,\{30\},n}, c_{2,\{30\},n}, \text{shift}_{\{30\},n}, \sigma^2_{\{30\},n})$ reflecting the posterior density, a sample $\xi_n \in \mathbb{R}^{30}$ reflecting the posterior predictive density can be obtained by the following computation:

- ▷ For $k \in \{1, \ldots, 29\}$, $\xi_n(k)$ will be the sum of $\Psi_{c_{1,\{30\},n}, c_{2,\{30\},n}}(v_{k,30})$ and a sample of a random variable with distribution $\mathcal{N}\big(0, \sigma^2_{\{30\},n}\big)$.
- ▷ Moreover, $\xi_n(30)$ will be the sum of $\frac{1}{\sqrt{2}}\big(g_{c_{1,\{30\},n}, c_{2,\{30\},n}}(t_1) + \text{shift}_{\{30\}}\big)$ and a sample of a random variable with distribution $\mathcal{N}\big(0, \sigma^2_{\{30\},n}\big)$.

The considered data vector is $\big(\psi_{1,30}, \ldots, \psi_{29,30}, \frac{1}{\sqrt{2}} L(t_1)\big)$. In Figure 12, the resulting violin-plots and the data vector values are shown.

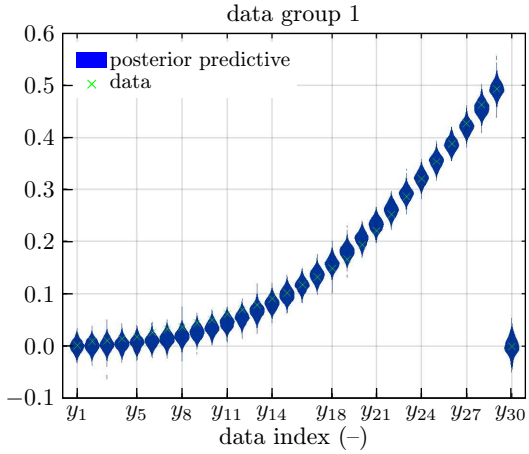

Figure 12. Violin-plots for the first data set with decreasing current, i.e. for data set No. 30, showing the posterior predictive density for the predicted values of the initial loading curve (data index $1, \ldots, 29$) and for $\frac{1}{\sqrt{2}}$ of the predicted length change at t_1 (data index 30).

4.7. Further results of Bayesian Inverse Problems for data sets with decreasing current. It was observed that for the data sets $22, \ldots, 29$ with decreasing current, i.e., the data sets $51, \ldots, 58$ in the complete numbering, the MCMC-scheme has not reached convergence or may not reach convergence. Hence, only the data sets for the first 21 data sets with decreasing current will be considered, i.e., the data sets $30, \ldots, 50$. A convex combination of the resulting posterior probability densities is approximated by randomly choosing some samples from each data set (number determined by some heuristic considerations involving the number of data points in the data sets), and afterwards merging all these samples to derive the *merged sample set for decreasing current*, see Figure 13.

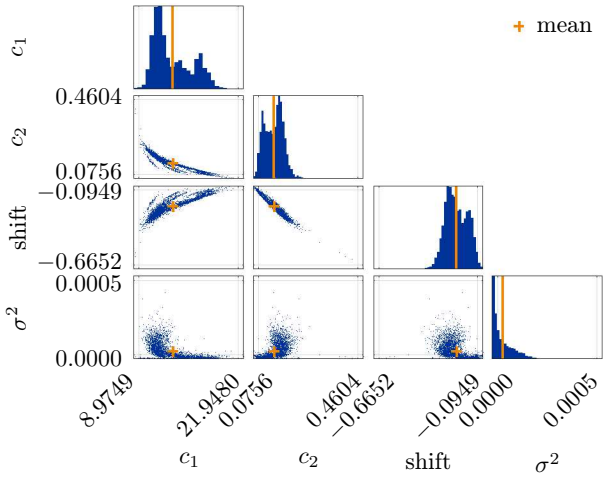

Figure 13. Scatter plot for a merged sample set for decreasing current.

4.8. Merging sample sets for data sets with increasing current and decreasing current. A number of samples are randomly chosen from the sample set considered in the last subsection, and the same number of samples are randomly chosen from the sample set for increasing currents, see Figure 7 and Figure 15. Afterwards, both these sample sets are merged, see Figure 14.

4.9. Result of forward UQ for merged data sets. In the following, one considers for every sample $(c_{1,n}, c_{2,n}, \text{shift}_n, \sigma_n^2)$ the function

$$[t_0, t_{58}] \ni t \mapsto \mathcal{G}_{c_{1,n}, c_{2,n}, c_3}[0, I](t) + \text{shift}_n$$

for the given value for c_3 and the trivial initial state. This generates a set of sample functions.

Now, for each of the time steps t in the measurement, sample values are created by performing the following computation for all considered n: the sample function number n is evaluated at t and $\sqrt{2}$ times a sample for a random variable with distribution $N(0, \sigma_n^2)$ is added.

Some quantile values are computed from the resulting samples for the posterior predictive density:

- ▷ the value of the 0.05—*quantiles at a time t* indicating that 5 % of all output sample values at time t are below this value and 95% are above this value,
- ▷ the value of the 0.95—*quantiles at a time t* indicating that 95 % of all output sample values at time t are below this value and 5% are above this value.

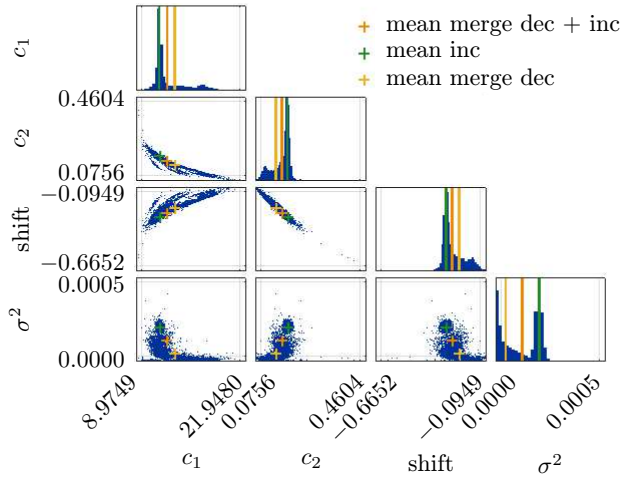

Figure 14. Samples derived by merging the samples for data sets with decreasing current, see Figure 13, and those for data sets with increasing current, see Figure 7 and also Figure 15. The means of theses sample sets are also shown.

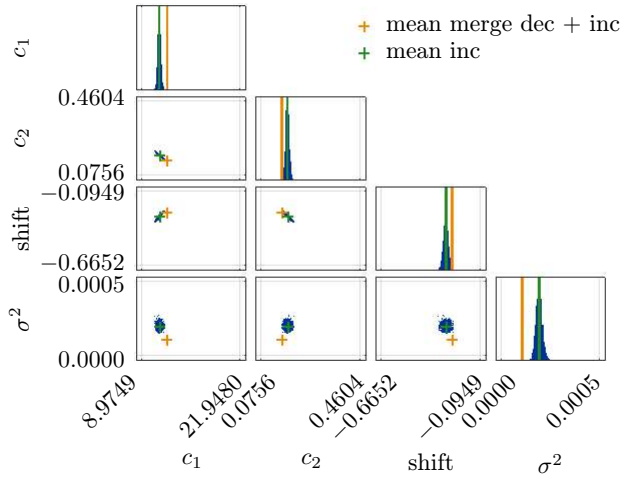

Figure 15. Scatter plot for the samples derived for 29 data sets with increasing currents is shown, and therein also the mean of these samples is also marked. These samples are also presented in Figure 7. In the current figure the intervals for plotting c_1, c_2, shift and σ^2 are the ones also used in Figure 14. Moreover, the mean of the samples shown in Figure 14, i.e., the merge of the samples for data sets with decreasing current and those for data sets with increasing current, is also marked.

In Figure 4, the measured data used for identification are shown. Now, the shown evolution of the measured length change in the identification period and the results of forward UQ can be compared, see Figure 16.

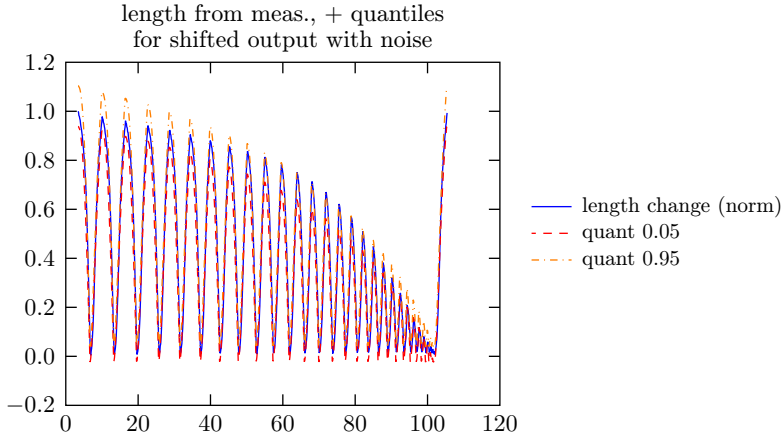

Figure 16. Result of forward UQ for merged data sets and measured length change during identification period.

Now, the evolution of the measured length change after the identification period and the results of forward UQ are also compared, see Figure 17 and Figure 18.

- ▷ For the period not used for identification with 210 data points it holds that for 61 data points, i.e., for **29 %**, the measured value is not in the interval [0.05—quantile value, 0.95—quantile value]. The values for 27 points are smaller than the 5%—quantile value and the values for 34 points are larger than the 95%—quantile value.
- ▷ For the period used for identification with 872 data points it holds that for 398 data points, i.e., for **46 %**, the measured value is not in the interval [0.05—quantile value, 0.95—quantile value]. The values for 182 points are smaller than the 5% quantile values and the values for 216 data points are larger than the 95% quantile values.
- ▷ Further investigations indicate that modeling using the generalized Prandtl-Ishlinskiĭ-operator produces a systematic error, somehow reflecting the systematic difference between the approximations for the initial loading curve for decreasing current and the corresponding approximations for increasing current.

4.10. Consequences of the result of forward UQ: Using the potential of the considered generalized Prandtl-Ishlinskiĭ-operator. The consideration in the previous subsection indicates that one may have to replace the generalized Prandtl-Ishlinskiĭ-operator in the model by another one.

FORC Diagrams are typically used to identify measures in so-called *Preisach-operators*, special kinds of hysteresis operators. In view of the model derivation in [3], Section 5, one should not use the generalized Prandtl-Ishlinskiĭ-operator to model the length change, but its *counterclockwise admissible potential* that is a Preisach-Operator. Then it holds that the generalized Prandtl-Ishlinskiĭ-operator $\mathcal{G}_{c_1,c_2,c_3}[\cdot,\cdot]$

should be used to model the magnetization. Reformulating the generalized Prandtl-Ishlinskiĭ-operator as a Preisach-Operator as in [3], Section 5 or [8], it follows that this corresponds to the situation of the next subsection with $\mu(r, v) = g_{c_1,c_2,c_3}(r, v)$ and

$$g_{c_1,c_2,c_3}(r,v) := \frac{c_1}{2}\exp\Big(\frac{-1}{2c_2}(\tanh(c_3(r+v)) + \tanh(c_3(r-v)))\Big) \times c_3^2 \tanh'(c_3(r+v))\tanh'(c_3(r-v)), \tag{4.15}$$

for all $r \geqslant 0$ and all $v \in \mathbb{R}$.

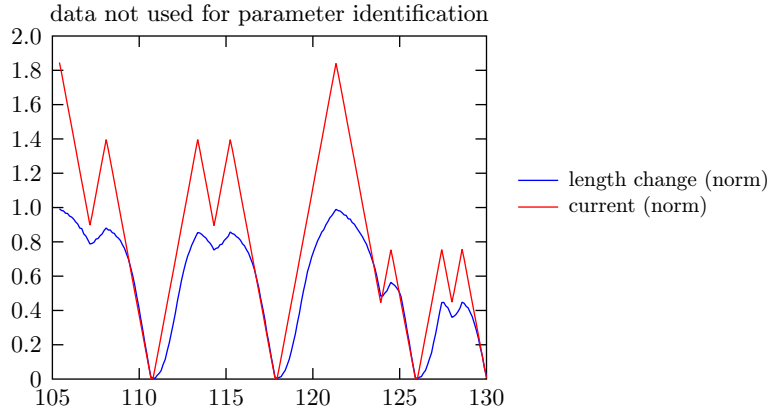

Figure 17. Evolution of current (input) and length change after identification period.

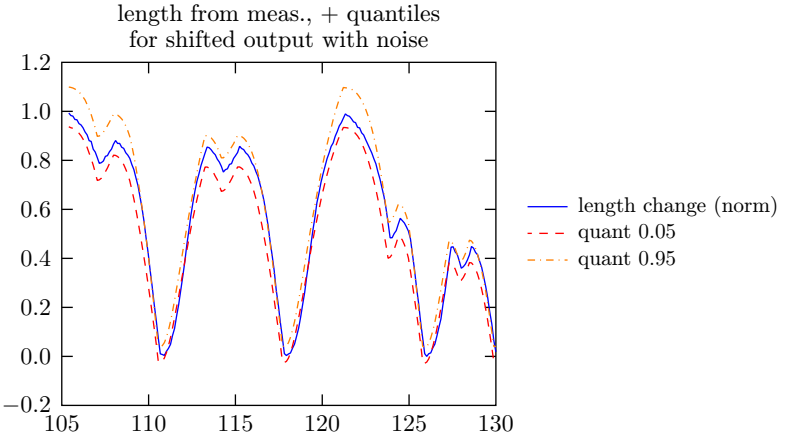

Figure 18. Result of forward UQ for merged data sets and measured length change, after identification period.

Some tests yield that using this operator generates a better approximation for the data generated for increasing current, but the approximation for the data generated for decreasing current time intervals gets worse, since the overfitting problem to the data sets for increasing current discussed in the next subsection takes place. Since

the data generated for decreasing current are the more relevant in this data set, it seems that one should consider some other operator instead and/or to derive an UQ-compatible way to reduce the overfitting problem.

4.11. Modifying model by using a general Preisach operator to model the magnetization and its potential to model the length change. In view of the last subsection, one would like to replace the potential of $\mathcal{G}_{c_1,c_2,c_3}[\cdot,\cdot]$ by another operator. To achieve this, one can consider [3], Section 5.1 and replacing there in the equation for the magnetization the generalized Prandtl-Ishlinskiĭ-operator by a general Preisach-Operator with a weight function $\mu\colon\ [0,\infty)\times\mathbb{R}\to\mathbb{R}$ see, e.g., [2], [10]. Therefore, it holds that the counterclockwise admissible potential should be of the form $\mathcal{U}_\mu[\cdot,\cdot]$ with

$$\mathcal{U}_\mu[\lambda_0,u](t) := 2\int_0^\infty \int_0^{\mathcal{P}_r[\lambda_0,u](t)} v\mu(r,v)\,\mathrm{d}v\,\mathrm{d}r \tag{4.16}$$

for all $u\in C([t_0,t_{58}];\mathbb{R})$, all λ_0 as in Definition 2.4, i.e., the Preisach-Operator with the weight function $(r,v)\mapsto v\mu(r,v)$.

In the following, it will no longer be assumed that the overall magnetic field H is proportional to the current I but that there may exist a further constant magnetic field H_0, maybe created by some permanent magnets, such that $H-H_0$ is proportional to the current I. Hence, some additional constant current I_0 is considered such that H is proportional to $I+I_0$ and $I+I_0$ is used as input function for the hysteresis operator in the following. (Such a modification would not have changed the results derived for the considerations with the generalized Prandtl-Ishlinskiĭ-operator in Section 3 and 4.)

Starting from the equation for the deformation in [3], (64), and adapting the considerations for dealing with the shift value in Section 4.2, one deduces that during the performed measurements it holds that

$$L(t)\approx \mathcal{U}_\mu[0,I+I_0](t)+\mathrm{shift} \tag{4.17}$$

for an appropriate function $\mu\colon\ [0,\infty)\times\mathbb{R}\to\mathbb{R}$ and appropriate values for $I_0,\mathrm{shift}\in\mathbb{R}$. The Everett-function $E_{\mathcal{U},\mu}\colon\ \mathbb{R}^2\to\mathbb{R}$ related to $\mathcal{U}_\mu[\cdot,\cdot]$ is defined by

$$E_{\mathcal{U},\mu}(\alpha,\beta) := \int_0^{(\alpha-\beta)/2}\int_{\beta+r}^{\alpha-r} v\mu(r,v)\,\mathrm{d}v\,\mathrm{d}r \quad \forall\,\alpha,\beta\in\mathbb{R} \text{ with } \alpha\geqslant\beta, \tag{4.18}$$

$$E_{\mathcal{U},\mu}(\alpha,\beta) := -E_{\mathcal{U},\mu}(\beta,\alpha) \quad \forall\,\alpha,\beta\in\mathbb{R} \text{ with } \alpha<\beta. \tag{4.19}$$

Considering an input function u and t_a,t_b,t_c as in Remark 2.6, one gets, analogously to (2.6),

$$E_{\mathcal{U},\mu}(u(t)+I_0,u(t_b)+I_0) = \frac{1}{2}(\mathcal{U}_\mu[\lambda_0,u+I_0](t)-\mathcal{U}_\mu[\lambda_0,u+I_0](t_b)) \quad \forall\,t\in[t_b,t_c]. \tag{4.20}$$

Using this and (4.17), one gets, analogously to (3.5) and (3.7), that one would like to find an appropriate function $\mu\colon [0,\infty)\times\mathbb{R}\to\mathbb{R}$ and an appropriate value $I_0\in\mathbb{R}$ such that

$$E_{\mathcal{U},\mu}(I(s_{k,l})+I_0, I(s_{0,l})+I_0) \approx \frac{1}{2}(L(s_{k,l})-L(s_{0,l})) =: \widetilde{\psi}_{k,l} \quad \forall\, k\in\{1,\dots,K_l^*\},\ l\in\{1,\dots,58\}. \tag{4.21}$$

On a first glance, is seems that one should follow the derivation of (4.1) and should assume that there are samples $\widetilde{\gamma}_{k,l}$ of independent random variables $\widetilde{\Gamma}_{k,l}$ such that

$$E_{\mathcal{U},\mu}(I(s_{k,l})+I_0, I(s_{0,l})+I_0)+\widetilde{\gamma}_{k,l} = \widetilde{\psi}_{k,l} \quad \forall\, k\in\{1,\dots,K_l^*\}, \quad l\in\{1,\dots,58\}, \tag{4.22}$$

and that the random variables $\Gamma_{k,l}$ have the distribution $\mathcal{N}(0,\sigma)$ for all $k\in\{1,\dots,K_l^*\}$ and for all $l\in\{1,\dots,58\}$ for an appropriate $\sigma>0$ that must be identified.

Considering now weight functions that are parameterized by parameters $\widetilde{c}_1$, $\widetilde{c}_2,\dots,\widetilde{c}_{\widetilde{M}}$, i.e., $\mu=\nu_{\widetilde{c}_1,\widetilde{c}_2,\dots,\widetilde{c}_{\widetilde{M}}}$, one could get the resulting likelihood for $(I_0,\widetilde{c}_1,\widetilde{c}_2,\dots,\widetilde{c}_{\widetilde{M}},\sigma)$ by considering the right-hand side of (4.2) with $\mathfrak{L}:=\{1,\dots,58\}$, K_l replaced by K_l^*, $\sigma_{\mathfrak{L}}$ replaced by σ, $\psi_{k,l}$ replaced by $\widetilde{\psi}_{k,l}$, and $\Psi_{\mathcal{PI},c_{1,\mathfrak{L}},c_{2,\mathfrak{L}}}(v_{k,l})$ replaced by $E_{\mathcal{U},\nu_{\widetilde{c}_1,\widetilde{c}_2,\dots,\widetilde{c}_{\widetilde{M}}}}(I(s_{k,l})+I_0, I(s_{0,l})+I_0)$.

Considering a further equation/further equations for shift derived from (4.17) and also a corresponding further factor for the likelihood, allows to generate a BIP and a corresponding likelihood. Now, using Bayes' theorem as in Theorem 3.4, one could get a formula for the resulting posterior density.

The numerical treatment of this problem would be more time-consuming than the one considered in Section 3 and 4, since further additional parameters with uncertainty have to be considered and one needs to use numeric integration to evaluate the Everett-function. For the same reasons, also the forward UQ would be costly.

But further investigations yield that one would have to modify the above considerations, since this approach would generate an overfitting to the data sets derived for increasing currents, i.e., the one for even l. It holds that

$$((s_{k,l})+I_0, I(s_{0,l})+I_0) \approx (I(s_{k,58})+I_0, I(s_{0,58})+I_0), \quad \widetilde{\psi}_{k,l}\approx\widetilde{\psi}_{k,58} \quad \forall\, l\in\{2,4,\dots,(58-2k)\}, \tag{4.23}$$

for all $k\in\{1,\dots,28\}$. Hence, it follows that the equations in (4.22) should only be considered for odd l and that one needs replacements for the equations for even l by some new equations that allow avoid/reduce overfitting in an UQ-compatible way.

To deal with general weight functions that would belong to some spaces with infinitesimal dimension, one would have to use a formulation of Bayes' Theorem appropriate for this situation, see, e.g., [18], Section 6.22, and dealing with this situations would be quite challenging.

If measurements $M(s_{k,l})$ for the magnetization were given, one could adapt the above considerations by using these values instead of $L(s_{k,l})$ and replacing in all integrals $v\mu(r,v)$ by $\mu(r,v)$.

4.12. UQ if the values for the initial internal states functions are of importance and also uncertain. The measurements used to generate FORC diagrams are usually performed in such a way that the involved differences are independent of the initial internal state of the operator and that the dependence can be reduced to dealing with a shift. In a general situation, the initial internal state λ_0 is influencing the evolution of L, e.g., (4.17) would be replaced by

$$L(t) \approx \mathcal{U}_\mu[\lambda_0, I + I_0](t) + \text{shift}. \tag{4.24}$$

If the values for the initial internal state function are uncertain, but in such a way that the function can be parameterized by a finite number of parameters and one has some probability density for the corresponding parameters and the parameters of the hysteresis operators, one can perform forward UQ by Monte-Carlo computations.

Moreover, if there are also some measurements for L up to some time $t^* > t_0$, one can formulate a BIP to use these measurements to update the considered probability density describing the parameter values that would allow to improve the prediction of the evolution of L after t^*. The appropriate formulation of the problem and the formulation of an appropriate numerical scheme would be a challenging task, where one would also have to decide between accuracy and velocity.

If the initial internal state is uncertain and cannot be parameterized, it would belong to some spaces with an infinitesimal dimension, and dealing with it would require some effort, see also the corresponding considerations in Section 4.11.

5. Conclusion

- ▷ Output of hysteresis operators depends on parameters whose values may not be exactly known when modeling real world processes.
- ▷ Inverse UQ to identify these parameters and their uncertainty has been performed.
- ▷ Forward UQ has been performed with the sample derived from inverse UQ; the results have been compared to measurements.

▷ The presented considerations have been performed for a magnetostrictive material, and a generalization of the considered model and possible fields of further research have been discussed. Of course, these considerations can also be adapted to deal with other models for materials with memory involving similar hysteresis operators.

6. Appendix

It holds, see, e.g., [17], Theorem 4.21 or [5], Exercise 4.9.3:

Lemma 6.1. *Let $(\Omega, \mathfrak{F}, \mathbb{P})$ be a probability space. Let $X_1, \dots, X_n \colon \Omega \to \mathbb{R}$ be independent continuous random variables such that there is some $\sigma \in (0, \infty)$ with $X_i \sim \mathcal{N}(0, \sigma^2)$ for all $i \in \{1, \dots, n\}$. Let $a_1, \dots, a_n \in \mathbb{R} \setminus \{0\}$ be given. Then it holds that*

$$\sum_{i=1}^{n} a_i X_i \sim \mathcal{N}\Big(0, \Big(\Big(\sqrt{\sum_{i=1}^{n} a_i^2}\Big)\sigma\Big)^2\Big) = \mathcal{N}\Big(0, \Big(\sum_{i=1}^{n} a_i^2\Big)\sigma^2\Big). \tag{6.1}$$

A c k n o w l e d g e m e n t. The author would like to thank Prof. Ciro Visone of the Università di Napoli Federico II, Napoli, Italy and Dr. Carmine Stefano Clemente and Prof. Daniele Davino of the Università degli Studi del Sannio, Benevento, Italy, for insights on the properties of magnetorestrictive materials and further fruitful discussion as well as for providing the experimental data investigated in this paper. The author would also like to thank Prof. Claudia Schillings, Freie Universität Berlin, Berlin, Germany, Prof. Tim Sullivan, University of Warwick, Coventry, United Kingdom, and Dr. Paul-Remo Wagner, ETH Zurich, Switzerland for fruitful discussions concerning UQ. Moreover, the author would like to thank Prof. Pavel Krejčí, Czech Technical University, Prague, Czech Republic for fruitful discussions concerning hysteresis and the referee for fruitful remarks.

References

[1] *M. Al Janaideh, C. Visone, D. Davino, P. Krejčí*: The generalized Prandtl-Ishlinskii model: Relation with the Preisach nonlinearity and inverse compensation error. American Control Conference (ACC). Portland, Oregon, 2014, pp. 4759–4764. doi

[2] *M. Brokate, J. Sprekels*: Hysteresis and Phase Transitions. Applied Mathematical Sciences 121. Springer, New York, 1996. zbl MR doi

[3] *D. Davino, P. Krejčí, C. Visone*: Fully coupled modeling of magneto-mechanical hysteresis through 'thermodynamic' compatibility. Smart Mater. Struct. *22* (2013), Article ID 095009. doi

[4] *D. Davino, C. Visone*: Rate-independent memory in magneto-elastic materials. Discrete Contin. Dyn. Syst., Ser. S *8* (2015), 649–691. zbl MR doi

[5] *G. Grimmett, D. Stirzaker*: Probability and Random Processes. Oxford University Press, New York, 2001. zbl MR

[6] *J. Kaipio, E. Somersalo*: Statistical and Computational Inverse Problems. Applied Mathematical Sciences 160. Springer, New York, 2005. zbl MR doi

[7] *O. Klein, D. Davino, C. Visone*: On forward and inverse uncertainty quantification for models involving hysteresis operators. Math. Model. Nat. Phenom. *15* (2020), Article ID 53, 19 pages. zbl MR doi

[8] *O. Klein, P. Krejčí*: Outwards pointing hysteresis operators and asymptotic behaviour of evolution equations. Nonlinear Anal., Real World Appl. *4* (2003), 755–785. zbl MR doi

[9] *M. A. Krasnosel'skij, A. V. Pokrovskij*: Systems with Hysteresis. Springer, Berlin, 1989. zbl MR doi

[10] *P. Krejčí*: Hysteresis, Convexity and Dissipation in Hyperbolic Equations. GAKUTO International Series. Mathematical Sciences and Applications 8. Gakkotosho, Tokyo, 1996. zbl MR

[11] *P. Krejčí*: Long-time behavior of solutions to hyperbolic equations with hysteresis. Evolutionary Equations. Vol. II. Handbook of Differential Equations. Elsevier, Amsterdam, 2005, pp. 303–370. zbl MR doi

[12] *P. M. Lee*: Bayesian Statistics: An Introduction. John Wiley & Sons, Chichester, 2012. zbl MR

[13] *S. Marelli, B. Sudret*: UQLab: A framework for uncertainty quantification in Matlab. Vulnerability, Uncertainty, and Risk: Quantification, Mitigation, and Management. American Society of Civil Engineers, Reston, 2014. doi

[14] *I. D. Mayergoyz*: Mathematical Models of Hysteresis. Springer, New York, 1991. zbl MR doi

[15] *M. Moustapha, C. Lataniotis, P. Wiederkehr, P.-R. Wagner, D. Wicaksono, S. Marelli, B. Sudret*: UQLib User Manual. ETH, Zürich, 2022; Available at `https://www.uqlab.com/uqlib-user-manual`.

[16] *Y. Pawitan*: In All Likelihood: Statistical Modelling and Inference Using Likelihood. Oxford Science Publications. Oxford University Press, Oxford, 2001. zbl

[17] *R. C. Smith*: Uncertainty Quantification: Theory, Implementation, and Applications. Computational Science & Engineering 12. SIAM, Philadelphia, 2014. zbl MR doi

[18] *T. J. Sullivan*: Introduction to Uncertainty Quantification. Texts in Applied Mathematics 63. Springer, Cham, 2015. zbl MR doi

[19] *A. Visintin*: Differential Models of Hysteresis. Applied Mathematical Sciences 111. Springer, Berlin, 1994. zbl MR doi

[20] *C. Visone, M. Sjöström*: Exact invertible hysteresis models based on play operators. Phys. B, Condens. Matter *343* (2004), 148–152. doi

[21] *P.-R. Wagner, J. Nagel, S. Marelli, B. Sudret*: UQLab User Manual: Bayesian Inversion for Model Calibration and Validation. ETH, Zürich, 2022; Available at `https://www.uqlab.com/inversion-user-manual`.

Author's address: *Olaf Klein*, Weierstrass Institute for Applied Analysis and Stochastics, Mohrenstr. 39, 10117 Berlin, Germany, email: `olaf.klein@wias-berlin.de`.